# High-Resolution Late Holocene Climate Change and Human Impacts on a Hypermaritime Peatland on Haida Gwaii, BC, Canada

**by**

**Matthew J. W. Huntley**

B.Sc., Simon Fraser University, 2009

Thesis Submitted in Partial Fulfillment
of the Requirements for the Degree of
Master of Science

in the
Department of Biological Sciences
Faculty of Science



**SIMON FRASER UNIVERSITY**

**Summer 2012**

# Approval

**Name:** **Matthew J. W. Huntley**

**Degree:** **Master of Science (Biology)**

**Title of Thesis:** ***High-Resolution Late Holocene Climate Change and Human Impacts on a Hypermaritime Peatland on Haida Gwaii, BC, Canada***

**Examining Committee:**

**Chair:** Dr. Tony Williams, Professor

---

**Dr. Rolf Mathewes**
Senior Supervisor
Professor

---

**Dr. Elizabeth Elle**
Supervisor
Associate Professor

---

**Dr. Marlow Pellatt**
External Examiner
Adjunct Professor, Department of Resource and Environmental Management
Simon Fraser University

**Date Defended/Approved:** May 23, 2012

## Partial Copyright Licence

## Abstract

A peat core from *Sphagnum*-dominated Drizzle Bog on Graham Island was used to identify factors that have influenced peatland development during the past ~1800 years. High-resolution paleoecological analysis included percentage and accumulation rate diagrams of pollen and other microfossils. $^{210}$Pb dates back to AD 1892 and four AMS radiocarbon dates provide a chronology of peat and microfossil accumulation back to AD 195. Few changes are evident before AD 1400 but a period of warm dry conditions is suggested by high pollen concentrations that coincide with high fire activity throughout the Yukon and Alaska. Low pollen accumulation between ~ 1600 and 1875 support cool growing seasons during the Little Ice Age (LIA). Dramatic increases in regional pollen productivity support rapid warming following the LIA after 1875. Construction of a gravel road through the bog in 1958 likely altered local hydrology as evidenced by changes in communities of rhizopoda and other organisms.



**Keywords**: Sphagnum; Little Ice Age; Haida Gwaii; Peat accumulation; Pollen accumulation rate; Industrial Period warming

## Acknowledgements

A project like this is never completed alone and I owe gratitude to many people as I near the end. Rolf Mathewes as my senior supervisor has been endlessly supportive and has provided insight into every aspect of this thesis. I am grateful to Elizabeth Elle for her (mild) edits and recommendations. I would also like to thank Marlow Pellatt as the public examiner for his fresh look at the project.

Thanks to our collaborator Bill Shotyk for sharing his expertise in geochemical and physical processes. I am also grateful to Nick Foit for his insight into microtephra and Olivia Lee at the UBC Herbarium for her moss identification skills. Credit goes to R. B. Worth for assisting with collection of the peat core.

Simon Goring and Bruce Archibald provided much-needed entertainment in our often-uninhabited lab. I would also like to thank members of the Elle lab, COPE lab and the SFU Biology grad community for providing much-needed distractions.

A special thanks to my parents for their support and Ivy Thompson for her endless patience and understanding.

# Table of Contents

# List of Tables

# List of Figures

## List of Acronyms

| | |
|---|---|
| AD | Anno Domini |
| BP | Before 1950 |
| MCA | Medieval Climatic Anomaly |
| LIA | Little Ice Age |
| IPCC | International Panel on Climate Change |
| BEC | Biogeoclimatic Ecosystem Classification |
| ENSO | El Nino/Southern Oscillation |
| PDO | Pacific Decadal Oscillation |
| CWH | Coastal Western Hemlock |
| MH | Mountain Hemlock |
| AT | Alpine Tundra |
| NPP | Non-Pollen Palynomorph |
| AMS | Accelerator Mass Spectrometry |
| PAR | Pollen Accumulation Rate |
| CONISS | Constrained Iterative Sum of Squares |
| SC | Similarity Coefficient |

## Quotation

“In dealing with the problems of cultural history the reconstruction of the history of nature should be considered a necessity.”

- Lennart von Post (1946, p. 217)

# 1. Introduction

## 1.1. Background

Haida Gwaii is an archipelago of ~180 islands off the west coast of Canada influenced by hypermaritime climate conditions, characterized by cool temperatures and high levels of precipitation. Like other coastal temperate areas, this climate encourages the formation of widespread oceanic peatlands. These unique ecosystems provide exceptional records of their development from biotic remains preserved within the peat. The anaerobic properties of peatlands allow for this preservation, impeding decomposition. Pollen and other microfossils are abundant and diverse and can be important tools in the reconstruction of changing paleoenvironments, including climate.

The use of pollen as an analytical proxy for vegetation composition was pioneered in the early decades of the 20$^{th}$ century. The Swedish geologist Lennart von Post is known as the father of quantitative pollen analysis as he perceived that pollen grains surviving in peat deposits had potential for studying past vegetation. He presented an analysis of pollen percentages plotted against stratigraphic position at a 1916 meeting of Scandinavian scientists in Oslo (Manten 1967). Nearly 100 years later and pollen percentage diagrams are still an important component in palynology used in conjunction with a number of methodological advances.

Some of the advancements in modern palynology include absolute pollen methods allowing for pollen taxa to be statistically independent from one another, such as pollen accumulation rates (Birks and Birks 1980). The use of stratigraphic units based on pollen flora using multivariate analytical techniques to define these pollen zones (Birks *et al.* 1975, Grimm 1987) is another advancement that helps with interpretation. The radiometric dating techniques, such as $^{14}$C (Piotrowska *et al.* 2011) and $^{210}$Pb (Le Roux and Marshall 2011), used to create accurate chronologies were unknown 100 years ago but are a necessity in modern palynological reconstructions. It is also common

to use multiple proxies in order to better understand biotic and abiotic processes in vegetation change (Booth and Jackson 2003; Chambers and Charman 2004; Birks and Birks 2006). There has also been an increasing interest in the role that climate plays in the development of vegetation communities, especially in peatland ecosystems (Barber 1981; Gignac 2001). Much like the research in von Post's time, the aim of modern palynological research is to further our understanding of past environments using as many of the tools at our disposal as is possible.

Modern Quaternary pollen analysis is guided by a number of principles and assumptions as outlined by Birks and Birks (1980) which are as follows: 1) pollen and spores are produced in large numbers during the reproductive stage of many plants; 2) pollen and spore proportions are dependent on the number of parent plants, thus reflecting the vegetation composition of an area; 3) many of these grains miss their mark and are deposited in environments conducive to preservation; 4) these microfossils can be extracted from sediment and identified to the family/genus/species level; 5) pollen and spores from different stratigraphic levels can provide information about vegetation from the different levels, and thus how vegetation changes over time.

The purpose of this study is to investigate a high resolution microfossil record from northern Graham Island, Haida Gwaii, British Columbia, Canada, in order to reconstruct vegetation and factors that have influenced bog development over the past ~1800 years. This period, known as the late Holocene, is well studied, but anthropogenic influences can often play a confounding role in interpretation. However, the Graham Island peatlands have relatively few human impacts due to Haida Gwaii's isolated location, with easy access to the region only developing in the latter half of the 20$^{th}$ century.

Peatland development is determined by three main influences; 1) vegetation succession, 2) changes in climate and 3) human-induced change (Blackford 2000). The reconstruction of local and regional vegetation from pollen and other microfossils should provide a detailed record of climate change and other disturbances during the past two millennia. The late Holocene is of particular international interest due to recent anthropogenic influences on our biosphere summarized in the International Panel on

Climate Change (IPCC): Assessment Report 4 (IPCC 2007). The IPCC describes key uncertainties for this time period that can be improved with more proxy data.

The objectives of this thesis were to (1) provide a high-resolution reconstruction of late Holocene peatland development from an oceanic *Sphagnum* bog through analysis of pollen and other microfossils; (2) investigate climate and other impacts on the regional vegetation and local peatland communities; (3) compare the findings of this study to other late Holocene studies in the region. The main emphasis of my research is focused on vegetation succession, apparent changes in regional productivity due to climate, and recent anthropogenic impacts influencing the bog community. The core that provided the data for this thesis was collected from Drizzle Bog on northeast Graham Island, BC, and is described in more detail in section 2.

## 1.2. Peatlands as Archives

### *1.2.1. Peatland Dynamics*

Terrestrial wetland ecosystems can be classified along a gradient determined by the influence of freshwater inputs. In general, those with high waterflow are richer in dissolved solutes while those with low freshwater flow tend to be nutrient poor. Peatland communities, also known as mires, are generally low-flow, nutrient poor wetland types and may be categorized as fens or bogs (MacKenzie and Moran 2004). Fens are dominated by graminoids (sedges and grasses) and experience some nutrient inputs from flowing groundwater supplemented by precipitation. Bogs are primarily ombrotrophic as nutrients are derived from atmospheric sources, namely precipitation and dust. The development of mires along temperate coasts is a gradual progression from rich fen to poor fen to raised bog (Gignac and Vitt 1990).

Peat accumulation ultimately controls the development of these communities and takes place whenever the net primary production at a site exceeds decomposition (Vitt 1994). This means that for peat to accumulate, growing seasons must be warm enough to encourage adequate plant growth but sufficiently wet to resist decay. High levels of precipitation in many coastal areas lead to the development of mire communities which are thought to be initiated by allogenic factors, namely levels of precipitation >500mm

per year (Gignac and Vitt 1994). This reliance on temperature and precipitation means that the accumulation of peat in these communities is at least in part influenced by climate.

### *1.2.2. Vegetation Succession*

The advanced successional stages of oceanic peatlands involving the transition from poor fen to raised bog are a focal point of this study. Poor fen peatlands are partially influenced by groundwater and experience only moderately acidic conditions with pH values between 4.0 and 5.5. Raised bogs differ due to dependence on rainwater and greater influences from *Sphagnum* that actively increase acidity resulting in pH values generally less than 4 (Vitt and Chee 1990).

There are few studies investigating fine-scale development of raised bogs of coastal sites on the Pacific north-west coast. Hebda (1977) investigated raised bog development of Burns Bog in Delta, BC, and proposed a model for raised bog development consisting of sedge-grass fen replaced by ericaceous shrubs and culminating in *Sphagnum* dominated raised bogs. Burns Bog is on the Fraser River Delta and Hebda suggests differences between this site and outer coastal peatlands. He mentions studies by Heusser (1955; 1960) who described a number of bogs along the west coast of Canada beginning with sedge peat and culminating in *Sphagnum* moss peat. In a similar study on the east coast of Canada, Auer (1930) describes maritime raised bogs in which sedge (*Carex*) layers are replaced by *Sphagnum* peat without any intervening shrub community.

A study by Quickfall (1987) investigated Holocene peatland initiation and development on Haida Gwaii. His study comprised 6 bog sites throughout the archipelago and one of his sites was Drizzle Pit (N 53.92567, W 132.10802), a peat exposure to the west of the Drizzle Bog core site investigated in this thesis. Quickfall describes the presence of a forest-fen complex following a paludification event at BP 4320 +- 100. This forest-fen patchwork was largely inferred due to the presence of rich fen species (*Carex obnupta* seeds) alongside woodland species (abundant *Pteridium aquilinum* spores). This patchwork was followed by increased concentrations of Ericales

and Cyperaceae pollen as well as *Sphagnum* spores, indicative of poor fen or bog conditions.

### *1.2.3. The Role of Sphagnum*

The late successional stages of peatlands are dominated by mosses of the genus *Sphagnum*. These peat mosses have a number of characteristics that allow them to restrict the growth of nearby vascular plants (van Breeman 1995; Rydin *et al.* 2006). They are known to form unfavourable environments for other plants in four ways: 1) limiting the availability of nutrients to other plants 2) creating anoxic conditions 3) reducing surrounding temperature as *Sphagnum* peat conducts heat poorly and 4) lowering the pH of the local substrate via cation exchange.

Not only can *Sphagnum* limit the growth of other plants but it has characteristics that allow it to thrive in peatland environments. *Sphagnum* mosses produce a number of phenolic compounds (Verhoeven and Liefveld 1997) which allow dead cell walls to resist decomposition. They lack true vascular tissue and use dead, decomposition resistant hyaline cells as a capillary network system (Moore and Bellamy 1973; Clymo and Hayward 1982), transporting water to the actively growing plant at the surface. In conjunction these two attributes are largely responsible for rapid peat thickening allowing peat to rise above the influence of groundwater, a process known as ombrotrophication.

The decomposition-resistant properties of *Sphagnum* along with anoxic mire conditions allow for the preservation of associated organic matter, including pollen and spores. Rapid peat accumulation and a lack of sediment mixing make raised bogs an ideal record for high-resolution studies of ecosystem dynamics. The assumptions inherent in using peats are that 1) microfossil remains are an accurate record of the bog community at the time of peat deposition and 2) reliable age estimates of the peat profile can be obtained using radiometric dating methods. An additional assumption arises when attempting to infer climate influences that 3) mire communities respond to changes in climate, primarily precipitation and temperature.

## 1.3. Late Holocene climate history

The oceanic islands of Haida Gwaii initiated their most recent period of peatland development ~ BP 5500 (Warner *et al.* 1984) during the cool, wet conditions of the mid-Holocene. Similarly, the study of several bogs in the area by Quickfall (1987) proposes peat initiation around BP 5000 in response to reduced temperatures and/or increased precipitation. The early stages in this peatland succession are well documented (Mathewes 1989) but the more recent, late Holocene development is poorly known.

The late Holocene is a period of relatively stable climate spanning the last ~ 3500 years (Walker and Pellatt 2003). Over this period the primary boundary conditions such as solar irradiance, orbital variations and ice sheet configuration, which influence global climate, are thought to be largely consistent with modern conditions (Walker and Pellatt 2003; Jones *et al.* 2009). The Drizzle Bog core spans most of the last two millennia. The most recent time period of this two thousand year interval is characterized by three sequential climatic phases. The 'Medieval Climatic Anomaly' spanning ~ AD 900-1450, the 'Little Ice Age' spanning ~ AD 1450-1875, and the industrial period from the late 19$^{th}$ century to the present. The timing and extent of these intervals varied among regions and discussion will focus on studies applicable to the Pacific Northwest coast. While it is unlikely that climatic conditions were static for the time before the Medieval Climatic Anomaly, the Drizzle Bog record does not record significant shifts prior to this time (see Chapter 5) so these conditions are not reviewed.

### *1.3.1. Medieval Climatic Anomaly*

The period preceding the 'Little Ice Age' has often been referred to as the Medieval Warm Epoch (Lamb 1995) or more commonly the Medieval Warm Period. Precipitation during this period was an important component of climate variability and for this reason a number of scientists have suggested the 'Medieval Climatic Anomaly' as a more appropriate term (Stine 1994; Bradley *et al.* 2003; Koch and Clague 2011). The duration and extent differ dramatically by region but generally conditions during the Medieval Climatic Anomaly were warmer and drier than those that immediately followed. There is little consensus on the exact timing but for the purposes of this study we define

the Medieval Climatic Anomaly as spanning from AD 900 to 1450 as per similar estimates by Bradley *et al.* (2003) and Herweijer *et al.* (2007).

Regional paleoclimatic studies are primarily restricted to tree-ring records and glacier maximal moraines. Glacier records from the St. Elias Mountains in southwest Yukon suggest warmer conditions from ~ AD 900-1490 that restricted glacier growth (Denton and Karlen 1973). Along the Northwest coast, tree-ring records reveal that two apparent multidecadal warm periods occurred centering around ~ AD 1300 and 1440 (Barclay *et al*. 1999).

### *1.3.2. Little Ice Age*

The 'Little Ice Age' (LIA) was a period of episodic cool climate events spanning from approximately AD 1450 to 1875 (Grove 1988; Fritz 2003). Multi-proxy studies suggest that the northern hemisphere experienced relatively cool mean temperatures from ~ AD 1450 to 1850 (Mann and Jones 2003). Ice core data from the Canadian High Arctic indicate that the coldest period of the entire Holocene was AD 1550 to 1900 with two particularly cold intervals of AD 1680-1730 and 1820-1860 (Bradley 1990).

Glacial records of Pacific coastal North America appear to display these LIA conditions with the expansion of glacier fronts in the St. Elias Mountains of southwest Yukon and Alaska from AD 1490 to 1920 (Denton and Karlen 1973). A review of British Columbia's glacial history by Menounos *et al.* (2009) suggests cool conditions throughout this period with a maximal regional ice coverage occurring between AD 1830 and 1880.

A coastal study of glacially overrun trees and the moraine formation of land-terminating glaciers around the Gulf of Alaska indicate glacial maxima at ~ AD 1650 to 1700 and final moraine stabilization around AD 1890 before glacier retreat began (Wiles *et al.* 1999). This date coincides with tree ring records in the same area of a multidecadal cold interval centered on AD 1870 (Barclay *et al*. 1999). Other coastal studies reveal that for several centuries during the LIA many of the glaciers near Bella Coola were at or near their maximum Holocene extent, reaching their maximal moraines between AD 1830 and 1880 (Desloges and Ryder 1990). A dendroglaciological study from the Todd Icefield north of Bella Coola, BC indicates two LIA expansions culminating

at ~ AD 1760 and 1900 (Jackson *et al.* 2008). The climate impacts at these coastal sites appear to end later than those of continental sites which are consistent with the findings of Luckman (1986) who found that the LIA appears to end later in the Coast Mountains than continental sites. To sum up these studies, cool periods from AD 1450 to 1875 appear to be influential to the region with two distinctive episodes culminating around AD 1700 and just before AD 1900.

### *1.3.3. Industrial Period*

The 20th century warming of global temperatures has been well-documented (Jones *et al.* 1999; IPCC 2007). Mann and Jones (2003) suggest that this recent warming is unprecedented at least as far back as AD 200 as displayed by current proxy records. They also indicate a gradual warming in the northern hemisphere after AD 1850 followed by a rapid increase in mean temperatures after AD 1890. This is consistent with the previously mentioned studies of various proxy reconstructions coming out of the LIA. Bradley (1990) suggests an increase in summer temperature after AD 1860 in his High Arctic ice core data. Glacial retreats in British Columbia become more frequent after AD 1880 (Menounos *et al.* 2009) and warm-season tree-ring reconstructions around the Gulf of Alaska suggest a warming following the AD 1870 cold interval (Wiles *et al.* 1996). In summary, the late 19th century displays a warming trend coming out of the LIA with accelerated warming throughout the 20th century.

# 2. Study Area

Haida Gwaii, formerly known as the Queen Charlotte Islands, is an archipelago of ~180 islands off the northwest coast of British Columbia (figure 2.1). The islands represent a small portion of the most expansive stretch of coastal temperate rainforest in the world. More than 1/3 of the global temperate rainforest grows along the western coast of North America, spanning from Alaska in the north to California in the south (DellaSala *et al.* 2011).

Haida Gwaii is also the most isolated island group in Canada, located on the western edge of the continental shelf, 50 to 150 km from the mainland. This isolation has earned it the moniker as the 'Canadian Galapagos,' an apt title given the number of evolutionarily distinct species and subspecies of plants and animals. Graham Island is the largest of the islands at over 6,000 $km^2$, and the main focus area of this study.

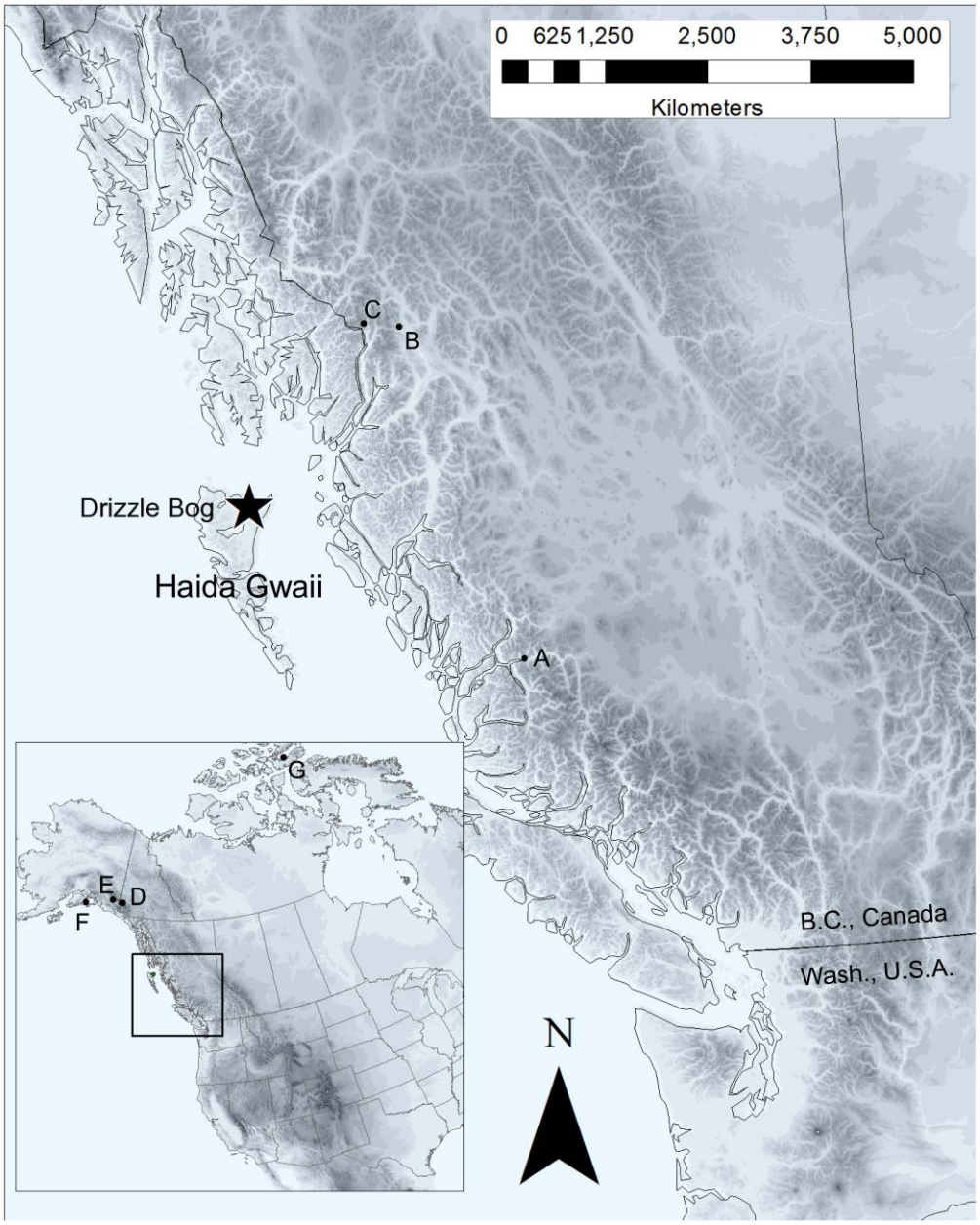


***Figure 2.1.*** ***Haida Gwaii map showing the location of the Drizzle Bog study site and the location of studies discussed in text. A) Bella Coola region (Desloges and Ryder 1990). B) Todd Icefield (Jackson et al. 2008). C) Tide and Summit Lakes (Clague and Mathewes 1996; Clague et al. 2004). D) St. Elias Mountains (Denton and Karlen 1973; Yalcin et al. 2006). E) Wrangell Mountain region (Davi et al. 2003). F) Western Prince William Sound and Gulf of Alaska (Barclay et al. 1999; Wiles et al. 1999; Calkin et al. 2001). G) Queen Elizabeth Islands including Ellesmere and Devon Islands (Fisher et al. 1983; Bradley 1990; Douglas et al. 1994). (Base map by Simon Goring, used with permission.)***

## 2.1. Regional Climate Drivers

The climate of the Northeast Pacific where Haida Gwaii is located is largely driven by two semi-permanent atmospheric pressure systems (Thomson 1989). The Aleutian Low is centered in the Gulf of Alaska and the North Pacific High is centered off the west coast of the United States. The North Pacific High predominates in summer (May through September) and its clockwise rotation results in north-to-northwesterly winds. During the winter (November through March) the North Pacific High is located closer to the equator and the counter-clockwise Aleutian Low is located farther south resulting in south-to-southeasterly winds. While the Aleutian Low and the North Pacific High are the main underlying climate drivers, they can be disrupted or enhanced by inter-annual cycles.

The two main atmosphere-ocean coupled inter-annual patterns that influence climate in the North Pacific are the El Nino/Southern Oscillation (ENSO) and the Pacific Decadal Oscillation (PDO). ENSO is a weakening of the trade winds resulting in warm water that would normally be piled up in the west Pacific, flooding across the Pacific basin to the west (Myles *et al.* 2005). During El Nino events which occur every 3-10 years, this warmer water can sometimes be as much as 1-2 °C above normal and appears on the outer British Columbia coast generally between October and June resulting in warmer than average winters. The opposite La Nina conditions are due to stronger than normal trade winds resulting in the opposite pattern and colder winters. The other inter-annual climate pattern, the Pacific Decadal Oscillation, has a similar spatial footprint to the El-Nino/Southern Oscillation. PDO events are on a longer time-scale than ENSO events as PDO warm/cool cycles each persist for ~20-30 years manifesting as a more frequent occurrence of El Nino events in warm PDO cycles versus La Nina event dominated cool cycles (Mantua *et al.* 1997).

## 2.2. Regional Setting

Since Haida Gwaii is situated on the extreme outer coast of British Columbia, it experiences high levels of precipitation from maritime air masses. The regional vegetation is dependent on these high rainfall levels and the wettest areas are prone to

the formation of peatlands. The result is a patchwork of open peatland, bog woodland and hypermaritime coniferous forest across the low-lying areas of Haida Gwaii.

Three Biogeoclimatic Ecosystem Classification (BEC) zones can be found on Haida Gwaii (Green and Klinka 1994), which are largely differentiated by elevation. The majority of Graham Island lies within the Coastal Western Hemlock (CWH) zone, which occurs up to 500-600m. Above this lies the Mountain Hemlock (MH) zone with small pockets of Alpine Tundra (AT) above ~800m.

These broadly classified BEC zones are further broken up into ecological variants depending on differences in climate and topography. Due to the location of the Queen Charlotte Ranges, precipitation is highest on the west side of Graham Island before air masses reach the eastern side, separating the island into the very wet hypermaritime variant west of the mountains (CWHvh2) and submontane wet hypermaritime variant to the east (CWHwh1) (Green and Klinka 1994). The Queen Charlotte Lowlands, which make up northeast Graham Island (figure 2.2), Drizzle Bog included, lie within the eastern CWHwh1 zone. The hypermaritime rainforests that make up the non-boggy portions of the CWHwh1 zone are a mixture of shore pine, Sitka spruce, western hemlock, western red cedar, and yellow cedar (*Pinus contorta* var. *contorta*, *Picea sitchensis, Tsuga heterophylla, Thuja plicata,* and *Callitropsis nootkatensis* respectively).

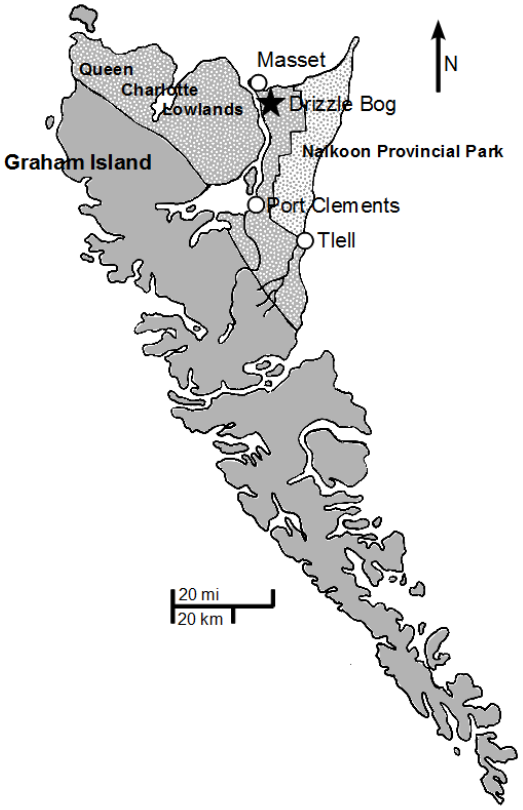


***Figure 2.2. Map of Haida Gwaii with regional areas of interest. Stippled area is the Queen Charlotte Lowlands while light stippling displays the margins of Naikoon Provincial Park.***

A considerable amount of rain still falls on the lowlands as indicated by Sewall Masset Inlet weather station (figure 2.3), which receives an average yearly precipitation of 1509 mm and experiences a temperate climate with a mean annual temperature of 8.2°C (Environment Canada 2011).

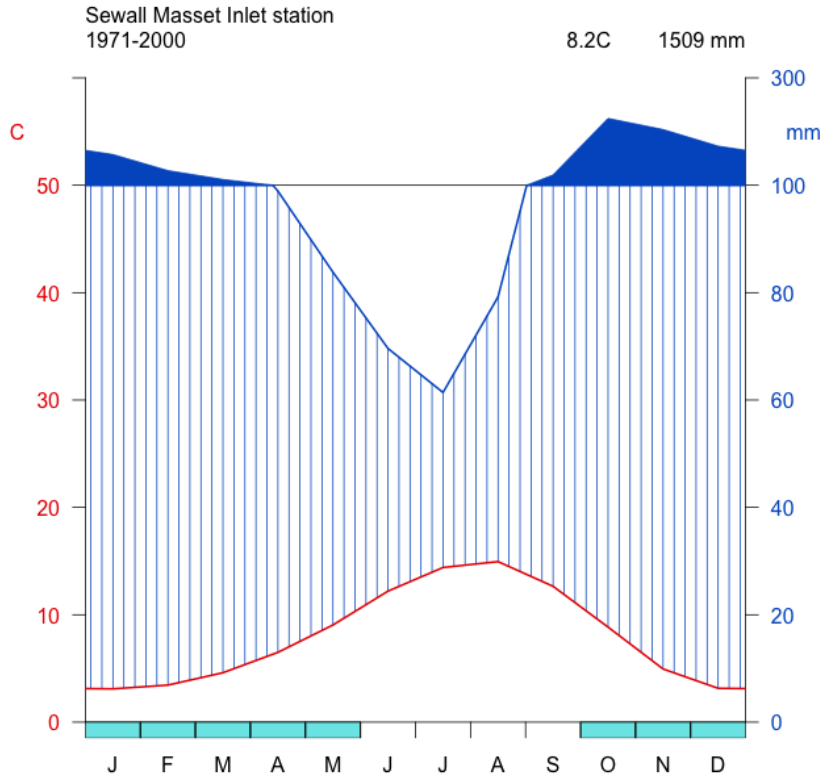


***Figure 2.3.*** ***Climatograph for Sewall Masset Inlet station using the 30-year average from 1971-2000 (Environment Canada 2011). Temperature scale (°C) is on left in red while precipitation scale (mm) is on right in blue. The precipitation scale changes from 20 mm intervals with blue vertical lines until 100 mm, where solid blue above displays precipitation between 100-300 mm on a compressed scale. Mean annual temperature and mean annual precipitation totals are displayed in top right. Climatograph generated using the climatol package (Guijarro 2011) in the statistical software program R (R Development Core Team 2011).***

## 2.3. Drizzle Bog Study Site

Drizzle Bog is located 10 km south of Masset, due west of the Naikoon Provincial Park boundary. It is an open *Sphagnum* peatland surrounded by hypermaritime forest and is crossed by Highway 16 on the southwestern edge (figure 2.4). The core was collected about 300 m northeast of the roadway at N 53.92772, W 132.10574. Argonaut Plain, to the northeast, is one of the largest unbroken expanses of peatland on the island and makes up a large part of Naikoon Provincial Park. As Drizzle Bog lies just outside of

the park, it shares many of the same vegetation and climatic characteristics of the peatlands within the park.


***Figure 2.4. Location of Drizzle Bog core site. A) Drizzle Pit site (Quickfall 1987). (Google Maps 2012)***

## 2.4. Drizzle Bog Site Vegetation

Drizzle Bog is a raised ombrotrophic *Sphagnum*-dominated peat bog. Ombrotrophic literally means ‘rain-fed’ and thus the vast majority of nutrient inputs come from atmospheric sources. It falls within the Shore pine – Black crowberry – Tough peat moss bog complex (Wb51), in the classification of Mackenzie and Moran (2004). The Wb51 bog type is extensive in and around Naikoon Provincial Park. Vegetation within this peatland complex is adapted to nutrient poor conditions and minerotrophic (groundwater-fed) species are generally absent. The surface vegetation is dominated by

*Sphagnum* mosses, with abundant ericaceous shrubs, sedges and other herbaceous plants, interspersed by stunted conifers (figure 2.5).

Tough peat moss (*Sphagnum austinii*) is a typical indicator species for the Wb51 bog complex and is one of the dominant hummock-forming peat mosses. *Sphagnum papillosum* is present at the site along with *S. andersonianum* and *S. rubelllum* which are commonly found on hummock sides. *S. magellanicum, S.lindbergii* and *S. angustifolium* are likely also present although positive identifications have not been made.

A number of ericaceous shrubs often colonize the tops of raised *Sphagnum* hummocks. The most frequently encountered is black crowberry (*Empetrum nigrum*) but *Rhododendron groenlandicum*, *Kalmia microphylla*, *Vaccinium uliginosum*, and *Vaccinium oxycoccus* are also present. Although not ericaceous, dwarf forms of common juniper (*Juniperus communis*) also grow scattered throughout the bog.

The herbaceous cover is dominated by sedges, mainly *Carex* and *Eriophorum* species, but a number of other flowering herbs are also present. Of these, *Cornus unalaschkensis*, *Rubus chamaemorus*, *Gentiana douglasiana*, *Drosera rotundifolia*, *Triantha glutinosa* and *Sanguisorba officinalis* were all present during the site survey in the summer of 2010. *Microseris borealis* is also common and is the only locally common Asteraceae species. As the survey was conducted in late summer, a number of herbaceous taxa that appear in the pollen record likely went unobserved due to earlier flowering times.

Shore pine (*Pinus contorta* var. *contorta*) makes up the majority of the stunted conifers growing on the bogs but Western Red Cedar (*Thuja plicata*), Yellow Cedar (*Callitropsis nootkatensis*) and Western Hemlock (*Tsuga heterophylla*) are also present.


***Figure 2.5. Drizzle Bog. A) View within Drizzle Bog near coring site. B) Wardenaar peat core being wrapped for shipping by my supervisor Rolf Mathewes. C) View of Drizzle Bog looking east from Highway 16.***

Scientific and common names of plant taxa identified from the pollen analysis and from the vegetation survey are shown in table 2.1. Most plant identifications were made from the author's knowledge in conjunction with Pojar *et al.* (1994) and Calder and

Taylor (1968). *Sphagnum* moss species collected at the site were identified by Olivia Lee at the University of British Columbia Herbarium. Taxonomic nomenclature for vascular plants follows that of the Integrated Taxonomic Information System (ITIS 2012).

***Table 2.1. Family, scientific and common names of plant taxa cited in pollen diagram or observed growing on the bog. Taxonomic nomenclature for vascular plants follows that of the Integrated Taxonomic Information System (ITIS 2012).***

| | Family | Scientific Name | Common name |
|---|---|---|---|
| **Trees** | | | |
| | Betulaceae | *Alnus* | alder |
| | Cupressaceae | *Callitropsis nootkatensis* | yellow cedar |
| | Cupressaceae | *Juniperus communis* | common juniper |
| | Cupressaceae | *Thuja plicata* | western red cedar |
| | Pinaceae | *Picea sitchensis* | Sitka spruce |
| | Pinaceae | *Pinus contorta* var *contorta* | shore pine |
| | Pinaceae | *Tsuga heterophylla* | western hemlock |
| | Pinaceae | *Tsuga mertensiana* | mountain hemlock |
| **Shrubs** | | | |
| | Empetraceae | *Empetrum nigrum* | crowberry |
| | Ericaceae | *Rhododendron groenlandicum* | labrador tea |
| | Ericaceae | *Kalmia microphylla* | western bog-laurel |
| | Ericaceae | *Vaccinium caespitosum* | dwarf blueberry |
| | Ericaceae | *Vaccinium oxycoccos* | bog cranberry |
| | Ericaceae | *Vaccinium uliginosum* | bog blueberry |
| | Myricaceae | *Myrica gale* | sweet gale |
| **Graminoids** | | | |
| | Cyperacaee | | sedges |
| | Poaceae | | grasses |
| **Herbs** | | | |
| | Apiaceae | | carrot family |
| | Asteraceae | *Microseris borealis* | apargidium |
| | Cornaceae | *Cornus unalaschkensis* | Western cordilleran bunchberry |
| | Droseraceae | *Drosera rotundifolia* | round-leaved sundew |

| | Family | Scientific Name | Common name |
|---|---|---|---|
| | Gentianaceae | *Gentiana douglasiana* | swamp gentian |
| | Menyanthaceae | *Nephrophyllidium/Menyanthes* | deercabbage |
| | Rosaceae | *Rubus chamaemorus* | cloudberry |
| | Rosaceae | *Sanguisorba officinalis* | official burnet |
| | Saxifragaceae | *Parnassia fimbriata* | Rocky Mountain parnassia |
| | Tofieldiaceae | *Triantha glutinosa* | sticky tofieldia |
| **Bryophytes** | | | |
| | Sphagnaceae | *Sphagnum andersonianum* | Anderson's sphagnum |
| | Sphagnaceae | *Sphagnum angustifolium* | fine bog-moss |
| | Sphagnaceae | *Sphagnum austinii* | tough peat moss |
| | Sphagnaceae | *Sphagnum lindbergii* | Lindberg's bog-moss |
| | Sphagnaceae | *Sphagnum fuscum* | Magellanic bog-moss |
| | Sphagnaceae | *Sphagnum papillosum* | Papillose bog-moss |
| | Sphagnaceae | *Sphagnum rubellum* | Red bog-moss |

## 2.5. Historic Site Impacts

The construction of a gravel road in 1958 (Leary 1982), connecting southern Graham Island with the town of Masset, likely altered local hydrology. Hydrological changes would have had a significant effect on floral and faunal communities of the bog. The initial gravel road was eventually paved in 1970 to become the westernmost end of the Yellowhead highway (Highway 16).

The introduction of a non-native vertebrate species is also a cause for concern with regards to local peatlands. Sitka black-tailed deer (*Odocoileus hemionus sitkensis*) were introduced to Graham Island in the early 1900s (Dalzell 1968), and are now the major large herbivore on the island. Since their introduction, deer overbrowsing has had a considerable impact on the structure of plant ecosystems, as there is no large predator, other than humans, to limit their numbers. Ericaceous shrubs such as salal (*Gaultheria shallon*) and red huckleberry (*Vaccinium parvifolium*), as well as bog

dwelling cloudberry (*Rubus chamaemorus*) have been declining on the island; these declines have been specifically attributed to an overabundance of deer (BC Parks 1992).

# 3. Methods

## 3.1. Core collection and vegetation description

The coring trip to Drizzle Bog was conducted in the summer of 2003. The 90 cm core was taken by Rolf W. Mathewes and R.B. Worth on July 14 (figure 2.5) using a 10 x 10 x 100 cm Wardenaar corer (Wardenaar 1987). The total peat depth at the coring site is 2.83 m, more than three times deeper than the depth of the core. Upon removal the core was wrapped in cling film and placed into a plastic-lined wooden case before being frozen and shipped to the University of Heidelberg, Germany for subsampling, geochemical analysis and Lead-210 dating, as per Givelet *et al.* (2004). A qualitative description of the local vegetation was also conducted at this time.

In August of 2010, a brief visit was conducted to describe the local vegetation cover. Two 20 m intersecting transects were established at the coring site. The first transect was oriented along a random compass bearing, with the second perpendicular to the first. 1 m x 1 m plots were assessed at 1 m intervals along each transect. The percentage cover of all identifiable species was recorded within each vegetation plot (Appendix 1).

## 3.2. Microfossil Analysis

### *3.2.1. Sample Preparation*

Initial processing of the frozen peat core was conducted by Dr. W. Shotyk and co-workers at the University of Heidelberg, Germany. Subsamples of 2 mL by displacement were taken at approximately 1 cm intervals from the 90 cm core and shipped to Simon Fraser University for pollen analysis. There, samples were prepared as per Faegri *et al.* (1989) using a modified standard preparation procedure that included HCl to remove calcium carbonates, KOH to remove humic acids and acetolysis

for the removal of cellulose. *Lycopodium* marker spores (11300 ± 400, Batch # 201890) were added to each sample prior to processing in order to calculate pollen concentrations. Samples were treated with hot 10% HCl and 10% KOH and topped up with distilled water before each centrifugation. Following KOH treatment the sample was decanted through a 250 µm brass sieve to remove coarse plant debris. Glacial acetic acid was used to remove water before samples were treated by acetolysis in a hot bath for 5 minutes. Samples went through an alcohol dehydration series in ethanol and finished with tertiary-butyl alcohol before being transferred to microvials with silicone oil. Slides were prepared by smearing residues with a toothpick to cover an area slightly smaller than the 22 mm cover slip. The cover slip was applied and nail polish was used to seal the edges.

### *3.2.2. Microfossil Counting*

Microfossil counts were performed at 500x magnification using a Zeiss research microscope (Model 47 30 12 - 9902). Critical identifications were made under oil immersion at 1250x magnification. A Coolpix 4500 digital camera with a photo tube attached to the microscope was used for all microfossil photographs. All microfossils of interest were identified and counted on each slide along regularly spaced transects. For each sample a minimum of one entire slide was counted with additional slides being counted as needed to reach an acceptable count total. Pollen sums included all terrestrial pollen types and all counts exceeded 450 grains with the majority exceeding 500 pollen grains. Of the 85 samples counted, 25 required the counting of an additional slide and 4 required a third. Pollen percentages for each sample were determined using the terrestrial pollen sum ($\Sigma P$) for each individual pollen type ($p$):

$$Pollen\ \% = \frac{p}{\Sigma P}\ x\ 100$$

All other identifiable microfossils were defined as non-pollen palynomorphs (NPPs). These included moss, fern and fungal spores, testate amoebae, copepod spermatophores and tardigrade eggs. The microfossil percentages were calculated in relation to the terrestrial pollen sum for each individual microfossil type ($m$):

$$Microfossil\,\% = \frac{m}{\Sigma P + m}\ x\ 100$$

#### 3.2.2.1. Pollen and Spores

Pollen and spore identifications were made using McAndrews *et al.* (1973), Moore *et al.* (1991), Kapp *et al.* (2000) and by comparison with the paleoecology lab reference collection at Simon Fraser University. Identifications to the species level were made where individual pollen grains could be positively identified or when the genus was only represented by one species within the study area. Scientific and common names of pollen types associated with the appropriate plant taxa are given in table 2.1.

A number of ericaceous plants grow on or near the site including a number of *Vaccinium* species, *Gaultheria shallon*, *Rhododendron groenlandicum*, and *Empetrum nigrum*. Of these species, the *Empetrum* and *Rhododendron* pollen tetrads are smaller (<30 µm) and generally more triangular compared to the larger (>40 µm), more spheroidal tetrads from the other local species (Figure 3.1). These observations are comparable to a study of the pollen morphology of Ericaceous plants from Burns Bog, British Columbia by Hebda (1979). Both *E. nigrum* and *R. groenlandicum* are associated with dry hummocks on coastal peat bogs, which justify splitting pollen identifications between *Empetrum/Rhododendron* and other undifferentiated Ericales pollen types for this study.

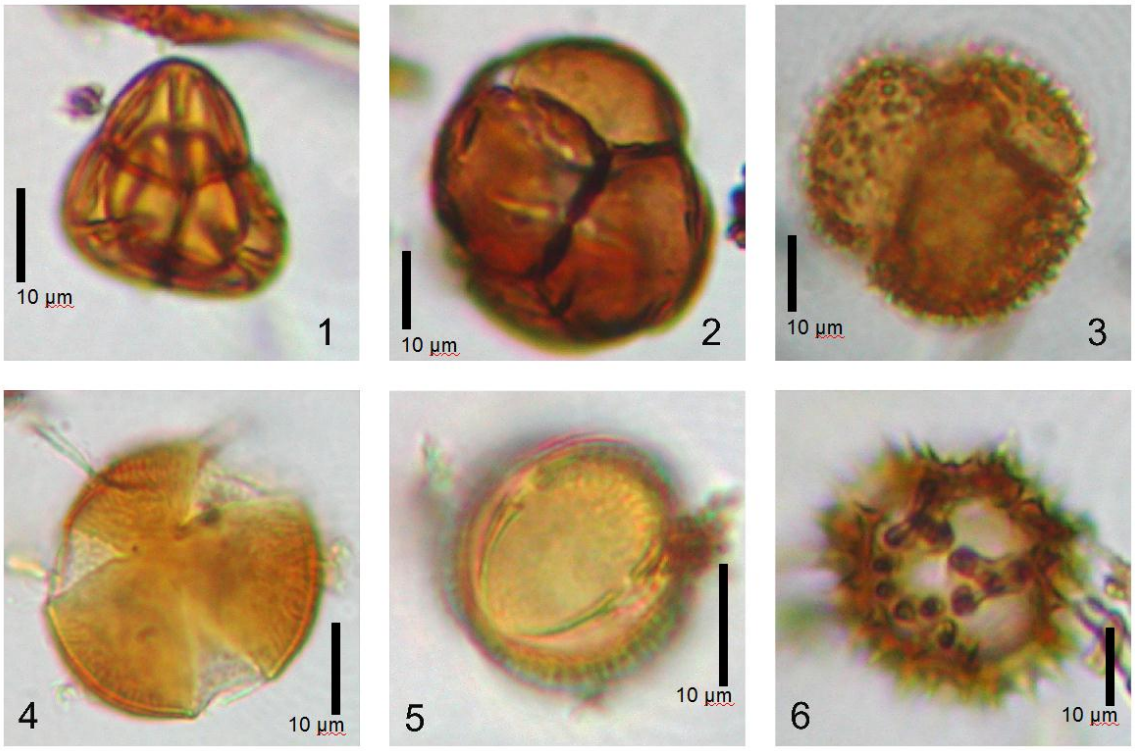


***Figure 3.1.*** ***Pictures from Drizzle Bog samples of select pollen discussed in text. 1) Empetrum/Rhododendron type 2) Ericales undifferentiated 3) Rubus chamaemorus 4) Nephrophyllidium/Menyanthes type 5) Parnassia fimbriata 6) Microseris borealis***

A preliminary analysis of *Sphagnum* spores was conducted in an attempt to differentiate between *Sphagnum* species or to improve paleoecological interpretation. Morphological references by Terasmae (1955), Tallis (1962) and McQueen (1985) were used but only *S.papillosum* and *S.rubellum* were described within. *Sphagnum* spores were collected at the Drizzle Bog site as well as from the University of British Columbia Herbarium. The *Sphagnum* species for which we were able to extract spores included *S.angustifolium, S.austinii, S.cuspidatum, S.lindbergii, S.papillosum, and S.rubellum.* Comparison of samples did not allow differentiation by species, as spore morphology was variable within taxa and the size range of spores overlapped between identified taxa.

### 3.2.2.2. Non-Pollen Palynomorphs

Other non-pollen palynomorphs, including testate amoebae and fungal spores, were also recorded (table 3.1). This allowed for a multi-proxy approach when analyzing the peat core for paleoenvironmental conditions.

***Table 3.1. Non-pollen palynomorphs (NPP) cited in NPP diagram and text with associated identification source***

| | Microfossil type | Identification source | Alternate name in citation |
|---|---|---|---|
| **Testate amoebae** | | | |
| | *Assulina seminulum** | (Payne *et al.* 2012) | |
| | *Assulina muscorum** | (Payne *et al.* 2012) | |
| | *Centropyxis* type | (Payne *et al.* 2012) | |
| | *Arcella discoides* type | (Payne *et al.* 2012) | |
| | *Arcella artocrea** | (Payne *et al.* 2012) | |
| | *Difflugia oblonga* type | (Payne *et al.* 2012) | |
| | *Amphitrema flavum** | (Payne *et al.* 2012) | *Archerella flavum* |
| | *Heleopera* type | (Payne *et al.* 2012) | |
| | *Trigonopyxis arcula** | (Payne *et al.* 2012) | |
| | *Euglypha* type | (Ogden and Hedley 1980) | |
| | *Hyalosphenia elegans** | (Payne *et al.* 2012) | |
| | *Nebela militaris* type | (Payne *et al.* 2012) | |
| **Fungal and other origin** | | | |
| | *Neurospora* cf. *reticulata* | (van Geel 1972) | type 1: Gelasinospora |
| | *Neurospora* cf. *retispora* | (van Geel 1972) | type 2: Gelasinospora |
| | cf. *Desmidiospora* | (Hebda 1977) | |
| | Type 18 ascospore | (van Geel 1972) | type 18 |
| | *Tilletia sphagni* | (van Geel 1972) | type 27 |
| | *Helicoon pluriseptatum* | (van Geel 1972) | type 30 |
| | Copepod spermatophore | (van Geel 1972) | type 28 |
| | Tardigrade egg type 1 | (Kinchin 1994) | *Macrobiotus* cf. *hufelandi* type |
| | Tardigrade egg type 2 | (Kinchin 1994) | *Macrobiotus areolatus* type |

* Testate amoebae positively identified to species level and thus included in NPP diagram

Testate amoebae, or rhizopods (Protozoa:Rhizopoda), are distinguished from other amoeboid protozoans by an external covering composed of secreted plates or inorganic particles (Taylor and Sanders 2001). These tests preserve well and often allow identification to the species level. Identifications were made using Ogden and Hedley (1980) and Payne *et al* (2012). In paleoecological studies, testate amoebae are useful indicators of change in hydrology and acidity within peatlands (Charman 2001). Species may occur in restricted ranges, both vertically and horizontally within the peat (Warner and Bunting 1996), thus providing information about local conditions. Only those taxa identified to species level were used in analysis (figure 3.2) as the taxa described as 'types' were in low abundance and there was some doubt in positive identification.

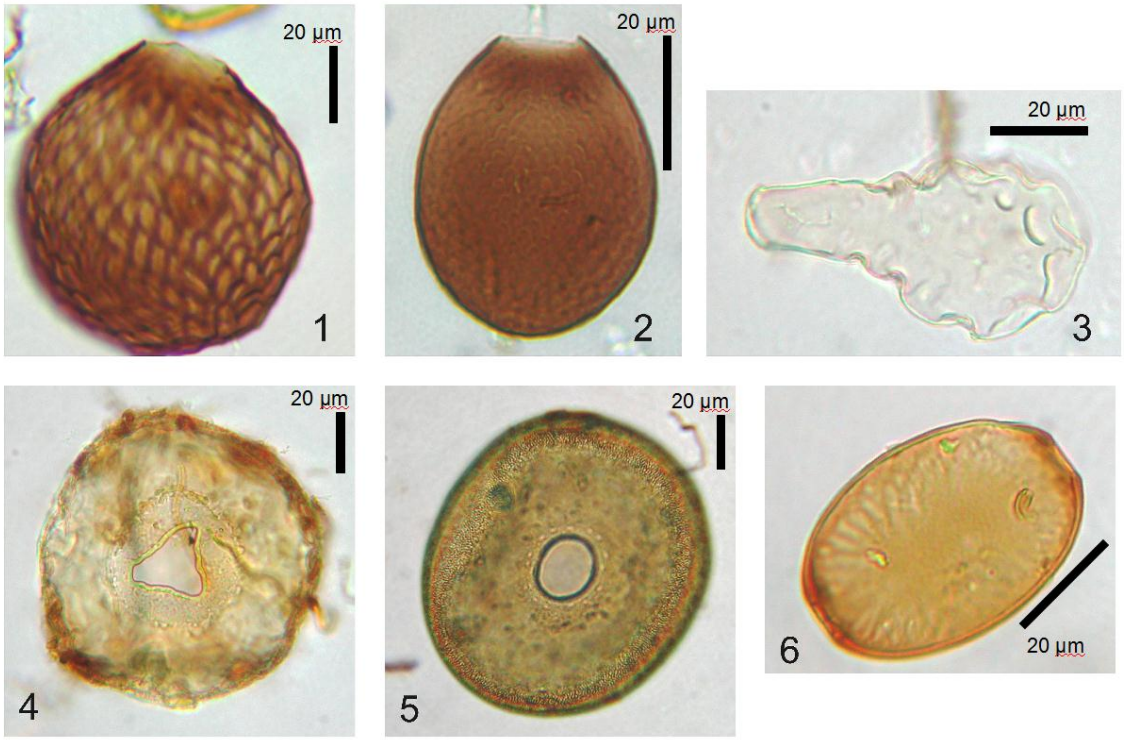


***Figure 3.2. Pictures from Drizzle Bog samples of testate amoebae discussed in text. 1) Assulina seminulum 2) Assulina muscorum 3) Hyalosphenia elegans 4) Trigonopyxis arcula 5) Arcella artocrea 6) Amphitrema flavum***

Fungal spores were identified using van Geel (1976), and his numbering of unknown microfossil types is used for comparison purposes (figure 3.3). The species ecology for fungi is largely unknown and their utility is mainly in associations with plant

remains and environmental conditions from other studies (van Geel 1976; Yeloff *et al*. 2007).

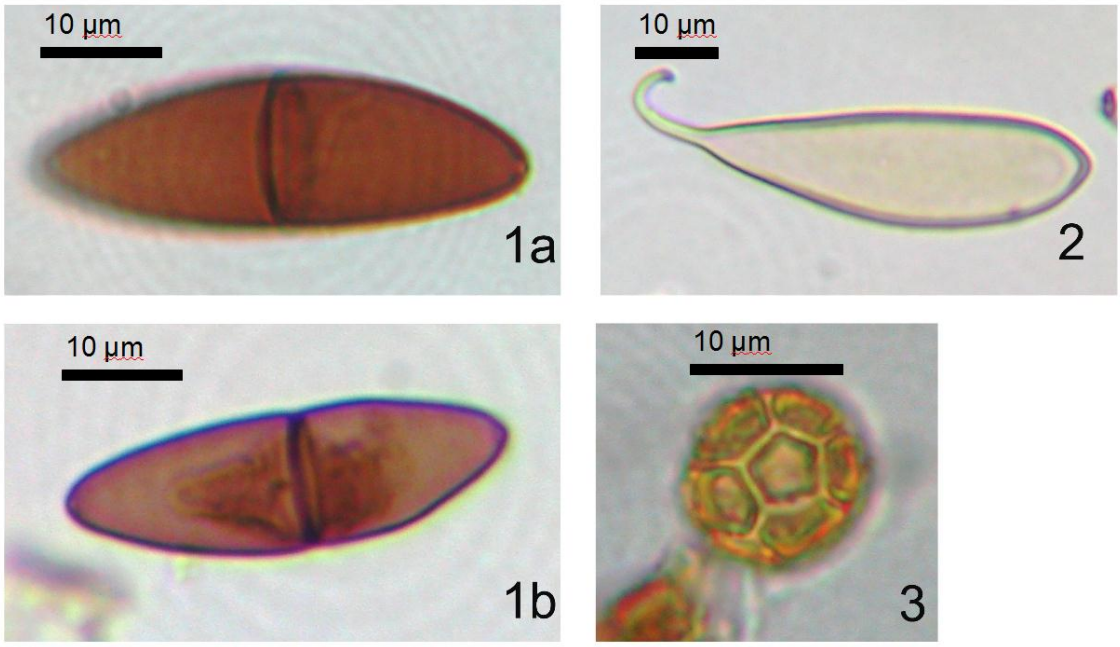


***Figure 3.3.*** ***Pictures from Drizzle Bog samples of other Non-Pollen Palynomorphs discussed in text. 1A) Type 18 fungal ascospore 1B) Type 18 fungal ascospore 2) Copepod spermatophore 3) Tilletia sphagni***

### 3.2.2.3. Macrofossils

*Sphagnum* branch leaf cells were investigated in an attempt to differentiate fossil species. Three leaf type identifications were able to be confidently determined: (1) *Sphagnum papillosum*, which is primarily found on poor fen lawns and to a lesser extent in raised bogs; (2) *Sphagnum austinii*, primarily found in raised bogs; (3) *Sphagnum* species from the Acutifolia section, which includes *S. andersonianum*, *S. fuscum*, *S. rubellum,* and *S. angustifolium,* most of which are found in both fen and bog communities. Though only a preliminary investigation was conducted, all three leaf types were present in the majority of the core.

## 3.3. Chronology

For this study 30 Lead-210 ($^{210}$Pb) dates (Table 3.2) and 4 radiocarbon ($^{14}$C) dates (Table 3.3) are used to construct an age-depth model (Figure 3.4). The $^{210}$Pb isotope has a half-life of 22 years and only those ages going back seven half-lives are distinguishable from background levels. Thus, only ages <150 years old are useful for construction of an age-depth model. Radiocarbon dating is limited in its age resolution within the last 150 years due to large uncertainties. The four radiocarbon dates span the interval between ~ BP 180 to 1800. The final $^{210}$Pb dates match well with the first of the radiocarbon dates.

$^{210}$Pb dates (n=30) were determined for each sample down to 31.2 cm by Peter G. Appleby from the Department of Applied Mathematics at the University of Liverpool as described in Appleby *et al.* (1997) and are listed in table 3.2. The constant rate of supply (CRS) model (Appleby and Oldfield 1978) was used, as the major assumption of an ombrotrophic peatland is such that the input of $^{210}$Pb is primarily atmospheric (Turetsky *et al.* 2004).

***Table 3.2. The $^{210}$Pb dates from the CRS model used for the chronological analysis of the Drizzle Bog core.***

| Depth (cm) | Dates from CRS model (yr AD) | Error (+/-) (yrs) |
|---|---|---|
| 0.00 | 2002 | 0 |
| 0.53 | 2000 | 2 |
| 1.59 | 1996 | 2 |
| 2.65 | 1992 | 2 |
| 3.71 | 1987 | 2 |
| 4.76 | 1982 | 3 |
| 5.82 | 1977 | 4 |
| 6.88 | 1972 | 5 |
| 7.94 | 1968 | 6 |
| 9.00 | 1965 | 6 |
| 10.06 | 1963 | 7 |
| 11.12 | 1960 | 7 |
| 12.18 | 1958 | 7 |
| 13.24 | 1955 | 7 |

| Depth (cm) | Dates from CRS model (yr AD) | Error (+/-) (yrs) |
|---|---|---|
| 14.29 | 1951 | 7 |
| 15.25 | 1947 | 7 |
| 16.41 | 1944 | 7 |
| 17.47 | 1941 | 8 |
| 18.53 | 1938 | 8 |
| 19.59 | 1935 | 8 |
| 20.65 | 1932 | 8 |
| 21.71 | 1929 | 8 |
| 22.76 | 1925 | 9 |
| 23.82 | 1921 | 9 |
| 24.88 | 1918 | 9 |
| 25.94 | 1913 | 10 |
| 27.00 | 1908 | 10 |
| 28.06 | 1904 | 10 |
| 29.12 | 1900 | 11 |
| 30.18 | 1895 | 11 |
| 31.24 | 1892 | 12 |

Four new radiocarbon dates are presented to help in the dating of the Drizzle Bog core (table 3.3.). Radiocarbon dates were determined using AMS (accelerator mass spectrometry) after acid-alkali-acid wash by Beta Analytic Inc. Calibrated ages were calculated in Oxcal 4.0 (Bronk Ramsay 2001) using the northern hemisphere terrestrial IntCal09 calibration curve (Reimer *et al.* 2009).

***Table 3.3. The four $^{14}C$ dates used for the chronological analysis of the Drizzle Bog core. Calibrated ages of the 2σ confidence interval have been included and converted to years AD and years BP. $^{14}C$ dates were measured by Beta Analytic Inc., Florida, USA***

| Material | | Depth (cm) | Dates ($^{14}C$ yr BP) | Calibrated Age (2σ (95%) yr AD) | (2σ (95%) yr BP) |
|---|---|---|---|---|---|
| *Sphaghnum* | Beta 228502 | 44 - 46 | 180 +/- 40 | 1650-1890 | 300-60 |
| Peat | Beta 283271 | 62 - 64 | 1170 +/- 40 | 770-980 | 1180-970 |
| Peat | Beta 228504 | 80 - 82 | 1590 +/- 40 | 390-560 | 1560-1390 |
| Peat | Beta 283272 | 88.4 - 89.5 | 1820 +/- 40 | 90-320 | 1860-1630 |

The age depth relationship was examined using a smoothed spline in the clam package (Blaauw 2010) within the statistical program R (R Development Core Team 2011) to combine the $^{210}$Pb age estimates with the $^{14}$C age estimates (figure 3.4). Point estimates were provided by the weighted mean of all age-model iterations (30,000) at each sample depth (Appendix C).

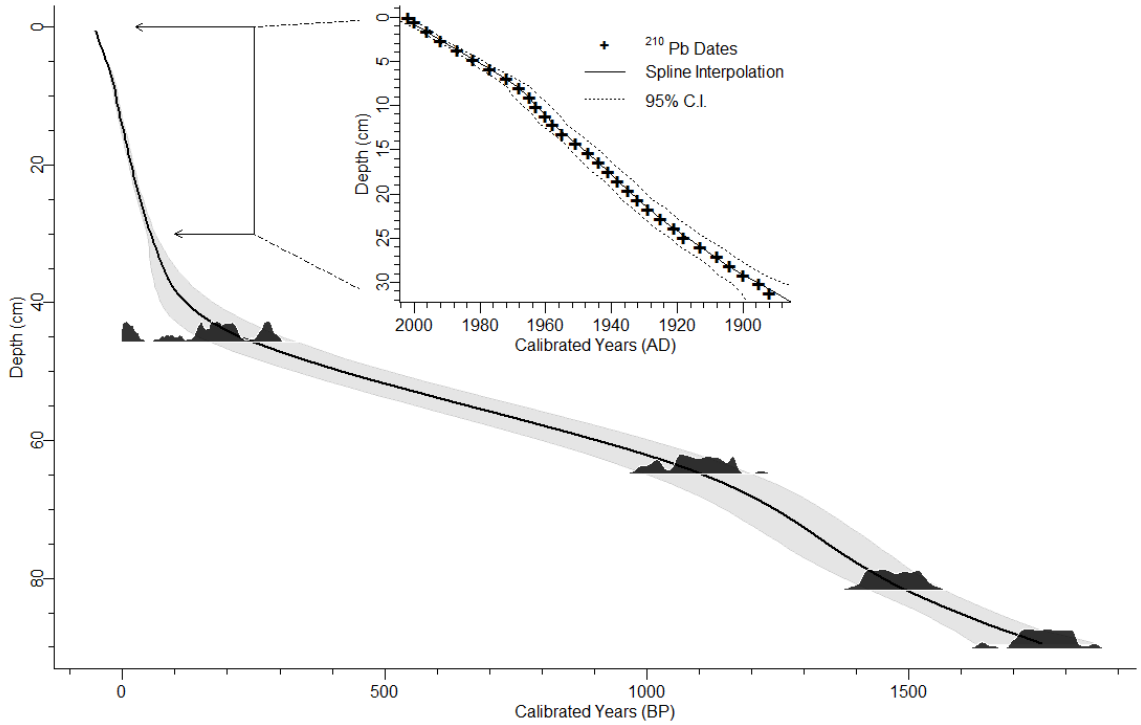


***Figure 3.4.*** ***Age-depth model of Drizzle Bog in calibrated years (BP) using a smoothed spline with the clam package (Blaauw 2010) in the statistical software program R (R Development Core Team 2011). The black line is the spline interpolation while the grey envelope shows the 95% confidence intervals based on 30,000 iterations. Black histograms represent calibrated curves for each of the four radiocarbon dates. Inset is the top 32 cm with the $^{210}$Pb dates in calibrated years (AD).***

## 3.4. Pollen Accumulation Rates and Sedimentation

Pollen diagrams can be displayed in several ways. The most common and standard method is a relative percentage diagram, which plots the percentage of each

taxon in relation to all other terrestrial pollen. Another method is an “absolute” pollen measure (Faegri et al. 1989) in which the abundance of each taxon is calculated independently from every other taxon. The pollen accumulation rate (PAR) is such a method, with all formulas generated as per Birks and Birks (1980). The PAR gives the number of pollen grains per unit surface area ($cm^2$) over a given length of time (1 year). Two separate lines of data are required to generate a PAR:

1) The pollen concentration ($P_{conc}$) within a known volume of peat (grains $cm^{-3}$):

$$P_{conc} = \frac{\Sigma P}{Marker\ spores\ counted}\ x\ Total\ marker\ spores\ added$$

2) The peat accumulation rate ($v$) as the net thickness of peat accumulated per unit time (cm $year^{-1}$):

$$v = \frac{Sample\ thickness}{\#\ of\ years\ per\ sample}$$

A process known as the exotic marker technique (Benninghof 1962) is used to satisfy the first requirement, in which a known number of marker spores are introduced to each sample prior to processing as mentioned in the previous section (3.1.2). This allows the analyst to determine the concentration of pollen taxa for each sample.

Another useful measure is the amount of time it takes (years) to produce a given unit of peat thickness (cm). This is the deposition time ($D$) and is the inverse of the peat accumulation rate (years $cm^{-1}$):

$$D = \frac{\#\ of\ years\ per\ sample}{Sample\ thickness}$$

With the pollen concentration ($P_{conc}$) from the exotic marker technique and the peat accumulation rate ($v$) using interpolated ages from the age-depth model we generate the Pollen Accumulation Rate (PAR; grains $cm^{-2}$ $yr^{-1}$):

$$PAR = P_{conc} \, x \, v$$

To generate the deposition time and peat accumulation rate necessitates an accurate chronology of the peat core. For the top 31 cm of the core we can be confident that the window of error is reasonably small as the resolution for $^{210}$Pb dates is relatively fine. Estimated ages lower in the core are dependent on radiocarbon dating which may not detect slight changes in accumulation rate. A combination of the percentage and PAR diagrams is thus necessary to fully interpret changes within the core.

## 3.5. Numerical Analysis

Both the pollen and the non-pollen palynomorph (NPP) diagrams were analyzed and plotted using TILIA v1.7 (Grimm 2011). Microfossil abundances were calculated for each sample as a percentage of the terrestrial pollen sum. The pollen diagram summarizes the frequency of pollen and spore taxa throughout the core. While all pollen types were used for numerical analysis only those taxa which have abundances >3% at some point are displayed in the diagram. For the NPP diagram, only the Accumulation Rate for each microfossil type was presented.

The Drizzle Bog core diagrams were subdivided into pollen zones and NPP zones based on the microfossil frequency data. These biostratigraphy zones were determined using stratigraphically constrained clustering. The use of these numerical methods permits identification of zones that are relatively independent of peat type, chronology, past vegetation or climate effects. This allows for the detection of changes to pollen or NPP assemblages in an unbiased way.

Stratigraphically constrained clustering using the incremental sum of squares (CONISS; Grimm 1987) was performed for both diagrams in which samples were grouped into clusters based on their similarity to adjacent samples. Square root transformation (Edwards and Cavalli Sforza's chord distance; Edwards and Cavalli-Sforza 1964) was applied to the microfossil percentage data in order to better represent rare taxa within the datasets. Using this method, three zones were discerned for each diagram.

## 3.6. Physical and Geochemical Analysis

Preliminary physical and geochemical analysis of the Drizzle Bog core was conducted by Nicolas Givelet between March 2004 and February 2005 at the University of Heidelberg, Germany. The physical and geochemical data was obtained by a collaborator, Dr. William Shotyk at the University of Alberta, for the purpose of investigating heavy metal deposition in peat. The only data used in this study was the peat bulk density and the ash content percentage. The bulk density is the dry mass per unit volume (g $cm^{-3}$) and was determined as per Givelet et al (2004). The ash content percentage is a measure of acid insoluble minerals within the peat. Peat samples were reduced to ash at 550 °C as per Steinman and Shotyk (1997) and treated with dilute HCl to remove carbonates and other inorganic components formed during the ashing process.

# 4. Results

## 4.1. Chronostratigraphy

Peat at 89-90 cm of the core is radiocarbon dated to 1820 ± 40 $^{14}$C yr BP which calibrates to a range of BP 1860-1630. The interpolated date from the age-depth model (figure 3.4) is BP 1754 (1856-1625) and thus the analyzed portion of the peat core spans approximately the last 1800 years. There are only minor changes in the rate of peat accumulation, with a particularly dramatic change at ~40 cm (BP 134 ± 55), just after the most recent radiocarbon date (180 ± 40 $^{14}$C yr BP). The peat accumulation rate rapidly increases after this point and the resolution of the core dramatically increases above 32 cm (BP 65 ± 15) due to radiometric $^{210}$Pb dates as is apparent in the age-depth model. The rate change is coincident with a change to well-preserved *Sphagnum* as the dominant component in the peat composition.

The temporal resolution for each ~1 cm sub-sample slice of the core is visually represented by the deposition time (figure 4.1 F) and averages just over 21 years. This average is meaningless in light of the dramatic difference above and below the major change in peat accumulation at 40 cm. The basal section of the core (90-40 cm) averages nearly 35 years per cm, ranging from 15 to 53.5 years. In comparison, the top section (40 cm to surface) ranges from 3 to 12.5 years, with a resolution averaging 4.6 years.

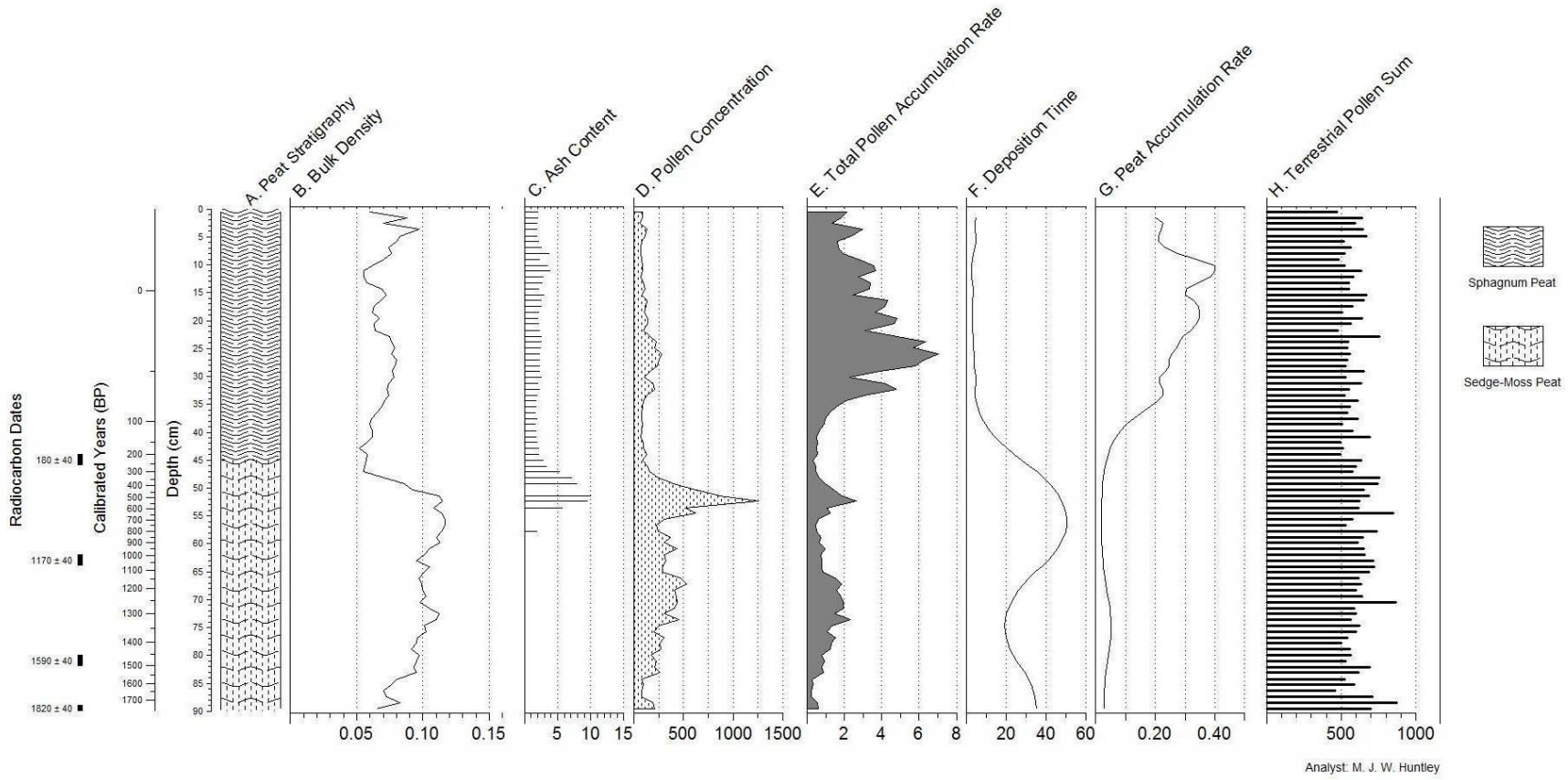


***Figure 4.1.*** ***Peat stratigraphy of Drizzle Bog core with physical and depositional measures A) Visual stratigraphy of the peat core. B) Bulk density for each sample in g $cm^{-3}$. C) The ash content % for a number of samples. D) The pollen concentration in # of pollen grains $cm^{-3}$ x 1000. E) The total Pollen Accumulation Rate in grains $cm^{-2}$ $yr^{-1}$ x 1000. F) Deposition time throughout the core in yr $cm^{-1.}$ G) The peat accumulation rate throughout the core in cm deposited per year. H) Terrestrial pollen sum for each sample.***

## 4.2. Peat Stratigraphy

This visual stratigraphy of the core indicates two zones (figure 4.1 A). The top half (0-45 cm) is a reddish-brown peat and is largely made up of *Sphagnum* moss remains. The darker, more humified bottom half (45-90 cm) is made up of more herbaceous material with significantly less *Sphagnum* remains. This visual differentiation in the core is emphasized by a dramatic change in bulk density.

The bulk density (figure 4.1 B) is a quantitative assessment of the peat composition and thus serves as a guide for most major changes apparent within the peat core. The most obvious event occurs at 52 cm where the bulk density displays an abrupt drop in density from around 0.10 g $cm^{-3}$ to just below 0.07 g $cm^{-3}$ in the top-most samples. The ash content percentage data (figure 4.1 C) was only available for a portion of the core but there is an apparent peak of 10% corresponding with the bulk density decline, much higher than the ~2% average for the rest of the core. Pollen concentration (figure 4.1 D) shows a dramatic increase at this 52 cm mark to over 125,000 grains $cm^{-3}$ before dropping to concentrations between 10,000 and 25,000 grains $cm^{-3}$, a lower concentration than was seen before the spike.

The only substantial changes within the peat core that do not appear tied to the bulk density are highlighted by the total Pollen Accumulation Rate (PAR; figure 4.1 E). Three periods of low PAR, which we describe as less than 1000 grains $cm^{-2}$ $yr^{-1}$, are apparent in the core. The PAR is low at the base of the core until 80 cm and is followed by the second low PAR period from 65 to 55 cm. The third low period follows 52 cm, spanning 49 to 37 cm. This final low PAR period is followed by a dramatic increase thereby reaching the highest rate of the core at 26 cm of over 6500 grains $cm^{-2}$ $yr^{-1}$ with a gradual decline before reaching ~2000 grains $cm^{-2}$ $yr^{-1}$ at the top of the core.

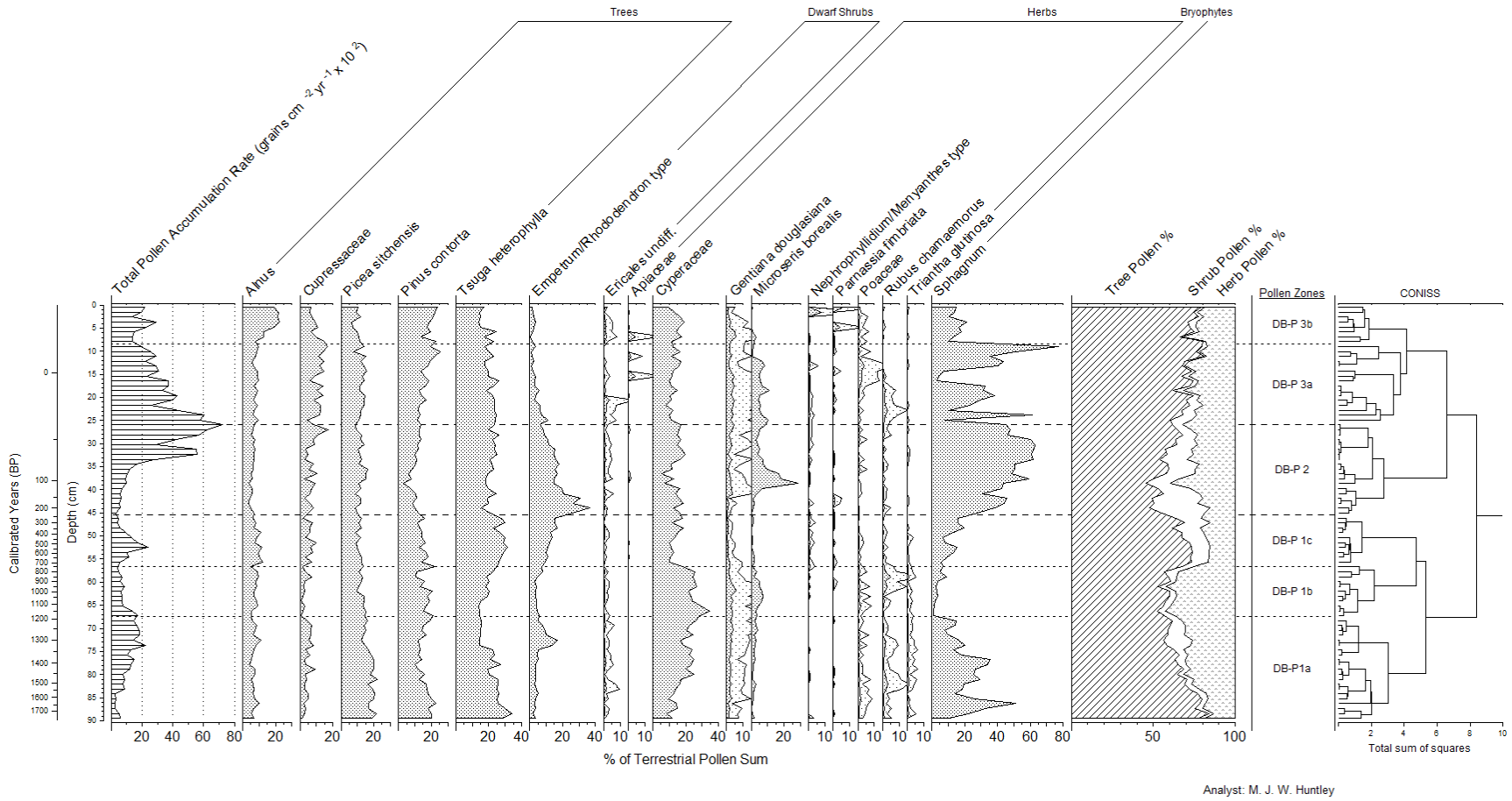


***Figure 4.2. Pollen percentage diagram of Drizzle Bog with pollen zones derived using CONISS. Stippling shows 5x exaggeration curves. The percentage of each taxon is in relation to the total terrestrial pollen sum for each sample.***

## 4.3. Pollen Analysis

### *4.3.1. Pollen Percentage Diagram*

The pollen diagram was divided into three main biostratigraphic zones (figure 4.2) using CONISS. Zone P-1 spans from 90 to 45.5 cm and is further divided into subzones P-1a, P-1b and P-1c, at 68 cm and 56 cm respectively. Zone P-2 begins at 45.5 cm up to 25.5 cm. Zone P-3 spans from 25.5 cm to the modern surface and is split into P-3a and P-3b at 8.5 cm.

**Pollen zone DB P-1 (90 to 45.5 cm)**

The lower half of the Drizzle Bog core makes up pollen zone P-1. *Sphagnum* spores in subzone P-1a frequently exceed 20% and reach as high as 50% of the total pollen sum. They are less abundant through subzone P-1b, reaching their lowest percentage of <10% before a gradual increase in subzone P-1c to over 20%. Cyperaceae pollen increases from ~10% at the base to around 25%, where it remains relatively constant until the start of subzone P-1c. This is followed by a notable decline in the percentage of Cyperaceae pollen at 57 cm from near 25% to <15% for the rest of the core. The *Empetrum*/*Rhododendron* pollen (figure 3.1) displays a short peak of ~15% to initiate subzone P-1b, up from <5% prior to, and immediately following the peak. By subzone P-1c, the percentage of *Empetrum*/*Rhododendron* pollen begins a gradual increase from <10%, to >20% by the end of zone P-1. *Microseris borealis* (figure 3.1) pollen reaches a small peak at ~5% midway through subzone P-1b, compared to averaging <1% before and after the subzone. Arboreal pollen percentages remain relatively constant throughout zone P-1.

**Pollen zone DB P-2 (45.5 to 25.5 cm)**

The marked increase in *Sphagnum* spore percentage along with the greater proportion of shrub and herbaceous pollen in relation to arboreal pollen are the dominant features of this zone. *Sphagnum* spores consistently make up over 50% of the total percentage. *Microseris borealis* pollen peaks briefly at >25% before dropping to ~7% by

the end of zone P-2 possibly indicating the sample included flowering remains. *Empetrum/Rhododendron* pollen displays a notable peak of >35% percent immediately following the 42 cm event before gradually declining over the course of zone P-2.

**Pollen zone DB P-3 (25.5 cm to surface)**

*Sphagnum* spore percentages display an erratic series of peaks and valleys before dropping to consistently remain at ~15% in P-3b for the duration of the core. *Empetrum/Rhododendron* percentages have also steadily declined after 45cm to < 5% in zone P-3. *Microseris borealis* pollen shows an average of 7% in P-3a before another notable decline to <1% within subzone P-3b. Pollen subzone P-3b is largely recognized by a doubling of *Alnus* pollen from a steady percentage of ~10%, throughout the core, to ~20%.

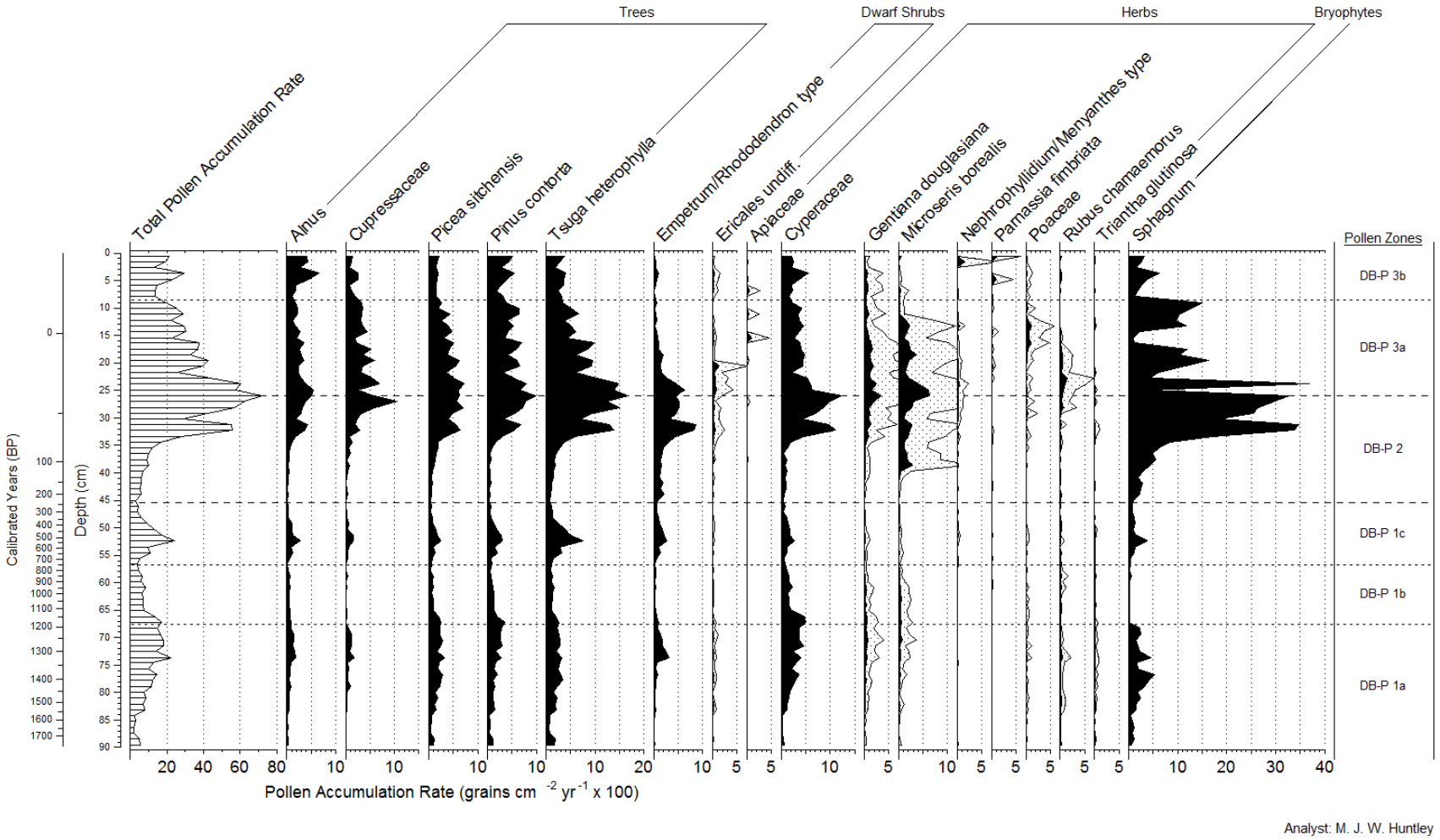


***Figure 4.3.*** ***Pollen Accumulation Rate diagram of Drizzle Bog with pollen zones. Stippling shows 5x exaggeration curves. The Pollen Accumulation Rate of all taxa is in grains cm$^{-2}$ yr$^{-1}$. Pollen zones are those generated by the CONISS dendrogram on the pollen percentage diagram (figure 4.2).***

### *4.3.2. Pollen Accumulation Rate Diagram*

The PAR diagram appears to describe a different picture than the percentage diagram. Looking at the total PAR makes this apparent as the percentage diagram only shows the proportional change of pollen in relation to other pollen types. The picture changes slightly when adding how many total pollen grains are deposited over time. Despite this dramatic difference, most taxa can be described by looking at the total PAR but a few patterns arise that differ from the percentage diagram. Pollen taxa that stand out will be investigated starting at the base of the core, moving forward in time.

The decline in Cyperaceae at the end of P-1b appears less dramatic in the PAR diagram when compared to the percentage diagram, yet Cyperaceae is still the most common pollen type early in the core compared to recent samples. The near absence of *Sphagnum* spores in P-1b becomes more evident in the accumulation rate diagram. A spike in *Tsuga heterophylla* at 52 cm is noticeable which was not immediately apparent from the percentage diagram. The *Empetrum/Rhododendron* increase immediately following the transition to P-2 is still relatively apparent. *Empetrum/ Rhododendron* pollen has a low accumulation rate at this time but in relation to other taxa many more pollen grains show up in the record*. Microseris borealis* pollen is present in small numbers throughout the core but appears to be quite productive throughout most of P-2 and P-3a before dropping out of the record almost entirely in P-3b. *Rubus chamaemorus* (figure 3.1) shows a similar pattern but is more constrained in time, peaking after the transition from P-2 to P-3a. *Gentiana douglasiana* nearly mirrors *M. borealis* but pollen is still apparent in P-3b. The *Alnus* increase part way through P-3b is evident in both diagrams suggesting a significant change in the regional vegetation.

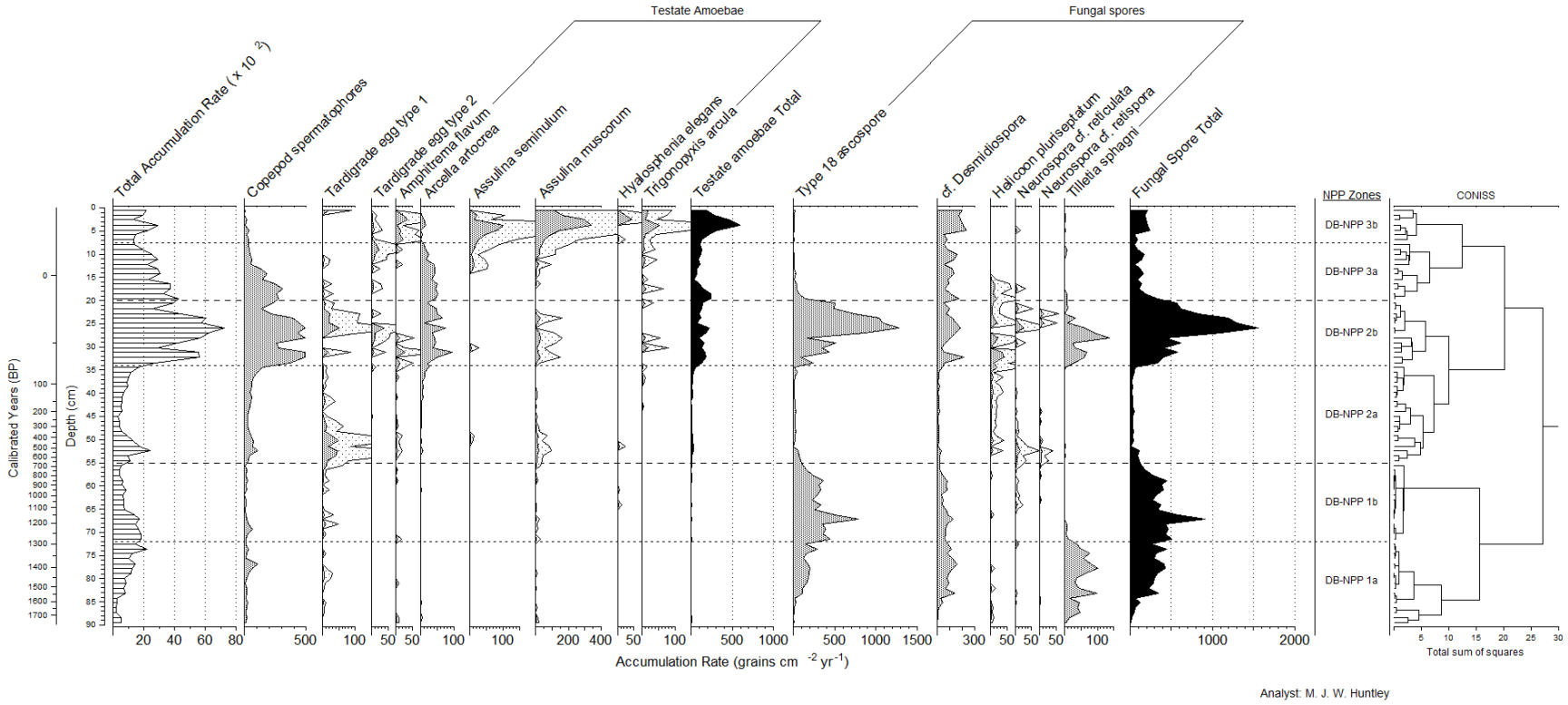


***Figure 4.4. Non-pollen palynomorph accumulation rate diagram of Drizzle Bog with CONISS. Accumulation rates are in grains $cm^{-2}$ $yr^{-1}$. Stippling shows 5x exaggeration curves.***

## 4.4. Non-Pollen Palynomorph Analysis

### *4.4.1. Non-Pollen Palynomorph Accumulation Rate Diagram*

Non-pollen palynomorphs (NPP) were divided up into three (3) main zones within the core (figure 4.4) and each zone was further divided into two subzones. Zone NPP-1 spans from the base of the core to 55 cm and is further broken into subzones NPP-1a and NPP-1b at 72 cm. Zone NPP-2 stretches from 55 cm up to 20 cm and is separated into NPP-2a and NPP-2b at 34 cm. The final zone of NPP-3 spans to the top of the core from 20 cm and is split into NPP-3a and NPP-3b at 7.5 cm.

**Non-pollen palynomorph zone DB NPP-1 (90 to 55 cm)**

A high proportion of fungal microfossils characterizes zone NPP-1, while all other NPPs are infrequent. *Tilletia sphagni* (figure 3.3) is present in relatively high numbers at the base of the core through to the start of subzone NPP-1b. The type 18 ascospores increase in abundance and commonly exceed 400 grains $cm^{-2}$ $yr^{-1}$ through NPP-1b before abruptly declining following the transition to zone NPP-2. Copepod spermatophores are present in low numbers while testate amoebae are particularly infrequent below 55 cm.

**Non-pollen palynomorph zone DB NPP-2 (55cm to 20 cm)**

Zone NPP-2 is characterized by a pronounced drop in most microfossil accumulation through subzone NPP-2a. Both *Neurospora* fungal types show an increase immediately following the initiation of zone NPP-2, though never in high amounts. At the 34 cm transition boundary to subzone NPP-2b is when we see an increase in the accumulation of most microfossil types. Rhizopod tests become more frequent with *Arcella artocrea* (figure 3.2) notably averaging more than 50 grains $cm^{-2}$ $yr^{-1}$. Of the fungal types, both type 18 and *T. sphagni* show dramatic accumulation increases peaking at over 1200 and 130 grains $cm^{-2}$ $yr^{-1}$ respectively. The final dramatic increase in microfossil accumulation is with copepod spermatophores, which average over 400 grains $cm^{-2}$ $yr^{-1}$ through the subzone.

**Non-pollen palynomorph zone DB NPP-3 (20 cm to surface)**

The defining feature of zone NPP-3 is the decline in accumulation of most fungal types at the 20 cm boundary. Copepod spermatophores also show this decline, though much more gradually. Rhizopod tests show similar accumulation rates as in subzone NPP-2b until a dramatic change is apparent at the boundary to subzone NPP-3b. All testate amoebae display their highest accumulation rates in this subzone with the exception of *Arcella artocrea*, which shows a marked decline. *Assulina seminulum* and *A. muscorum* (figure 3.2) are the most notable, displaying peaks of 100 and 340 grains $cm^{-2}$ $yr^{-1}$ respectively.

## 4.5. Comparison of Pollen zones to Non-Pollen Palynomorph (NPP) zones

The boundaries between the zones generated from the CONISS dendrograms of the pollen and non-pollen microfossils are not always at similar depths, although they are relatively close in time (Figure 4.5). Discrepancies between different proxies are unsurprising since there is a difference in how climate and other factors affect the organisms of each microfossil group. For the pollen taxa a large proportion represents regional pollen rain from the surrounding area. While bog conditions play a role in structuring the local vegetation, all plants are influenced by regional climatic factors as well. The non-pollen palynomorphs however are primarily the remains of animals that are influenced by local bog conditions, and not regional conditions. These animals are comparatively short lived and their abundance changes immediately to different conditions within the bog.

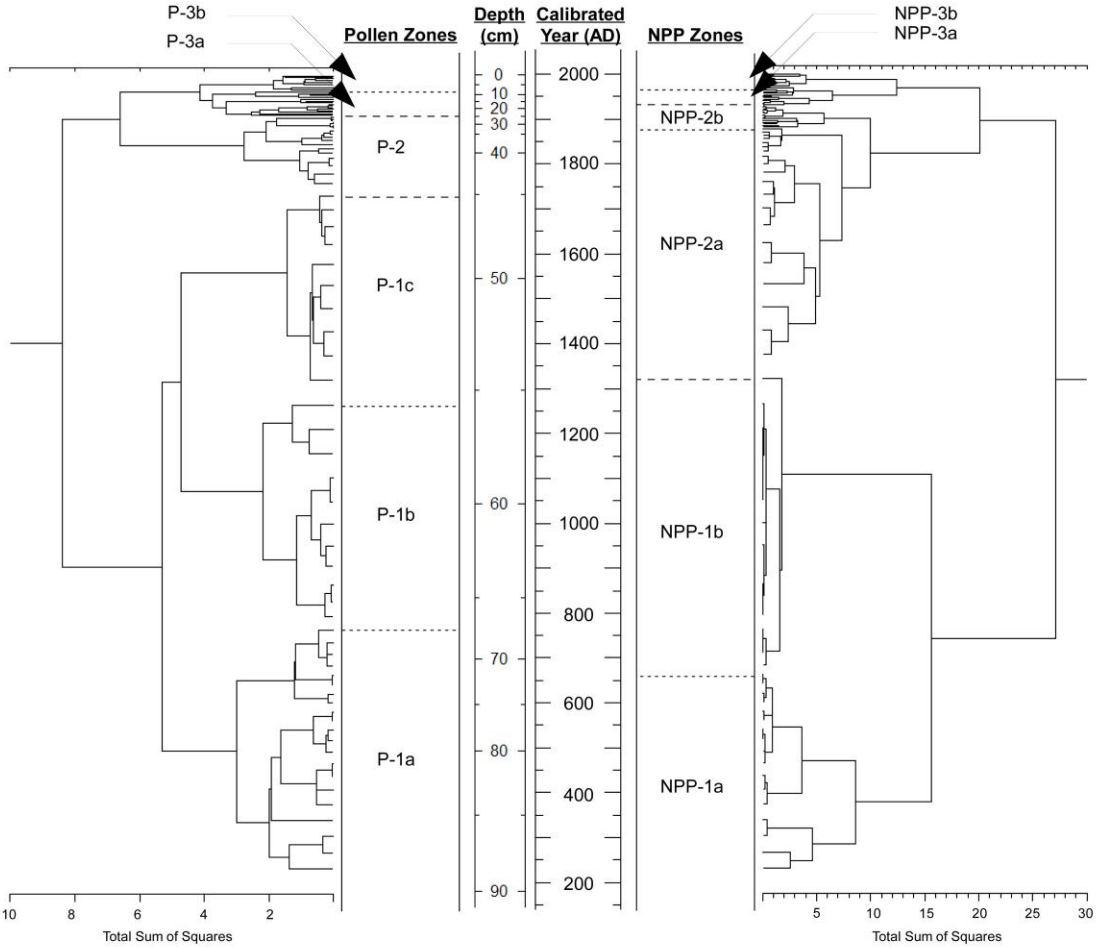


***Figure 4.5. Chronological comparison of Pollen CONISS dendrogram zones on the left and Non-Pollen Palynomorph CONISS dendrogram zones on the right.***

The boundary between P-1a to P-1b at AD 770 (BP 1180) follows ~100 years after NPP-1a to NPP-1b at AD 660 (BP 1290). The next boundaries are even closer at a difference of ~50 years, with NPP-1 to NPP-2 at AD 1310 (BP 640) and P-1b to P-1c at AD 1260 (BP 690). The subsequent boundaries for pollen and non-pollen palynomorphs are the only ones that do not match up closely with P-1 to P-2 occurring at AD 1720 (BP 230) and NPP-2a to NPP-2b occurring at AD 1875 (BP 75). The boundaries closest to present day match up surprisingly well between pollen and NPP. The boundary at P-2 to P-3 at AD 1915 (BP 35) occurs ~20 years before the NPP-2 to NPP-3 boundary at AD 1935 (BP 15). The most contemporary boundaries only differ by ~5 years with P-3a to P-3b occurring at AD 1965 (BP -15) and NPP-3a to NPP-3b occurring at AD 1970 (BP -20).

# 5. Discussion

## 5.1. Peatland Succession

At the base of the core, the vegetation and microfossil assemblages suggest a sedge-dominated mire with a large component of *Sphagnum* mosses. Cyperaceae is the most abundant pollen type for much of the lowermost zone P-1 as seen in the PAR diagram (figure 4.3), exceeding even *Sphagnum* spores for the majority of the bottommost zone. In terms of proportion Cyperaceae makes up over 20% of all pollen until 57 cm. The microfossil assemblage indicates that the peatland may have been a poor fen-type with more of a sedge and herbaceous vegetation component than is apparent later in the core. It should be noted that mires are defined along a gradient and that poor fen and raised bog types share much of the same plant species. It seems reasonable that Drizzle Bog may already have been transitioning from a poor fen to a raised bog near the base of the core, as *Sphagnum* spores were already abundant and there is no apparent loss of species subsequently. The *Sphagnum* mosses that were present may have been a mixture of mesotrophic species, not necessarily contiguous with the modern *Sphagnum* assemblage.

The bulk density of the mire (figure 4.1) at this earlier stage also suggests a sedge-moss composition due to its higher bulk density (Chambers *et al.* 2011). This assessment is supported when compared to Chambers *et al.*'s (2011) analysis of the bulk density of different peat types in western Canada. They found that the median bulk density of sedge-moss peat was 0.098 g $cm^{-3}$ (interquartile range of 0.08-0.12 g $cm^{-3}$) while the median bulk density of *Sphagnum* moss peat was 0.067 g $cm^{-3}$ (interquartile range of 0.05-0.09 g $cm^{-3}$). The bulk density of the Drizzle Bog core is a near match to these peat type differentiations, suggesting a sedge-moss peat composition with 0.099 g $cm^{-3}$ lower in the core until 50 cm followed by *Sphagnum* dominated peat with a bulk density of 0.068 g $cm^{-3}$. This sedge-dominated peat is also suggested by the high abundance of type 18 fungal ascospores, which are often associated with *Eriophorum*

species as they correlate with periods of high Cyperaceae pollen abundances (van Geel 1976).

A near absence of *Sphagnum* spores in subzone P-1b (67.5 to 55 cm) is slightly puzzling (figure 4.3). One possibility is that this period highlights a transition from mesotrophic *Sphagnum* species associated with poor fen mires to oligotrophic species associated with raised bogs. However, there is little support for this hypothesis other than a lack of spores in subzone P-1b as the bulk density does not decline until after 50 cm. Poor fen species are also generally present in coastal ombrotrophic mires (Gignac *et al.* 1991) so a more likely explanation is that climatic conditions were not conducive to spore production in *Sphagnum* species. This scenario of low PARs due to climatic factors is further discussed in section 5.3.

The diffuse boundary between the two visual stratigraphic zones around 45-50 cm is suggestive of a recurrence surface. A recurrence surface by definition is the boundary separating slow peat growth identified by higher humification, followed by fresh, actively growing *Sphagnum* peat (Birks and Birks 1980). The actual depth of the recurrence surface appears to be at 52 cm as determined by the pollen concentration peak of >125,000 grains $cm^{-3}$, followed immediately by a bulk density change. The pollen at this point is over twice as concentrated as any other point in the core, implying an important change in mire dynamics. This pollen concentration spike likely indicates very little to no peat accumulation suggesting a prolonged dry period at around BP 550 (AD 1400 ± 100).

During prolonged dry periods the peat dries out, encouraging aerobic decomposition. If decomposition is equal to or greater than net primary production at the surface peat growth can halt, functionally resulting in a hiatus in peat accumulation. The spike in content percentage at 52 cm (figure 4.1 C) indicates this as the only component remaining after organic material decomposes is the mineral components present within vegetation. If the vegetation that normally contributes to peat accumulation decomposes one would expect a high proportion of acid insoluble minerals compared to organic material, displayed by the ash content spike.

The 52 cm depth is also the only point in the core where both *Neurospora* fungal types (figure 4.4) are consistently present for any length of time, though in small quantities. The presence of *Neurospora* has been attributed to locally dry conditions in other analyses of bog stratigraphy (van Geel 1972; Yeloff *et al.* 2007) supporting this proposed dry period.

Immediately following 52 cm we see a dramatic increase in peat accumulation. This high rate of peat growth suggests a transition to a raised bog with strictly ombrotrophic inputs. *Sphagnum* moss has become the dominant mire species as evidenced from the bulk density change (figure 4.1) and pollen diagrams (figures 4.2 and 4.3). After substantial proportions early in the core followed by their near absence in subzone P-1b, *Sphagnum* moss spores begin a rapid proportional increase following the recurrence surface. It should be noted that a gradual reduction in peat accumulation rate lower in the core would be expected due to compaction but is unlikely to be as abrupt as is shown at the recurrence surface.

### *5.1.1. Testate Amoebae as Indicators*

Of the testate amoebae identified to the species level, the majority can occupy a wide range of hydrological conditions within *Sphagnum* mosses. For this reason these testate amoebae are known as sphagnicolous rhizopods (Glime 2007). All of the identified tests are from sphagnicolous taxa and their increased presence after the recurrence surface also support the transition to a raised *Sphagnum* bog.

Only a few taxa appear to occupy specific enough conditions to be useful in determining local environments. Other identified taxa can tolerate a comparatively wide range of conditions within the *Sphagnum* peat environments. The most useful species, *Arcella artocrea*, tends to occupy very wet peat conditions indicative of a high water table and is the only identified taxon reportedly found in open water (Payne *et al.* 2012). The opposing hydrological indicator taxa, *Trigonopyxis arcula*, are suggestive of dry conditions with a lower water table (Tolonen *et al*. 1992; Booth 2001). The dramatic increase in all identified rhizopod taxa, with the exception of *Arcella artocrea*, defines subzone NPP-3b and highlights an important change in the peatland micro-community likely caused by human impact.

## 5.2. Anthropogenic Impacts

### *5.2.1. Road Construction*

The only anthropogenic disturbance that appeared to impact the mire community was the relatively recent construction of Highway 16 to the southwest of the coring site. The initial gravel road connecting Port Clements to Masset was finished in AD 1958 (BP - 8; Leary 1982), and was later paved in 1970, becoming the westernmost terminus of the Yellowhead Highway. The construction of this highway across the western edges of Drizzle Bog coincides with the final CONISS sub-zone boundary for both pollen and non-pollen palynomorphs (figures 4.2 and 4.4). While the construction itself likely influenced the local community, improved human access to this formerly inaccessible area also appears to have influenced the regional pollen composition through logging.

The initial gravel road, finished in 1958, corresponds to a depth of 12 cm in the core. This depth is slightly before both the pollen (P-3b at 8.5 cm) and NPP (NPP-3b at 7.5 cm) subzones begin but some significant shifts in NPP are apparent at this time. The presence of copepods is an indicator of standing water (Anderson 1998) and the decline of their spermatophores after this 12 cm mark may indicate a lowering of the water table. The only rhizopod taxon that is reported to live in open water is *Arcella artocrea* whose presence and subsequent decline mirrors the copepod spermatophore abundance at the same stage in the core. The high abundance of type 18 ascospores may also indicate the presence of standing water as this fungal spore is commonly found in the presence of *Eriophorum* species (van Geel 1976). Both species of *Eriophorum* (*E. chamissonis* and *E. angustifolium*) found on Haida Gwaii can tolerate a wide range of wet substrates but are commonly found around the margins of ponds (Aiken *et al.* 2007). The large quantity of these three microfossil types together suggest wet conditions prior to the decline of all three to near absence following the road construction in 1958 (12 cm).

There are currently culverts running underneath the road which may allow the northeastern areas to drain resulting in the loss of pooling water. The increase in most other rhizopod taxa at this point may be a result of this reduced water table as well. The lowering of the water table would allow for more *Sphagnum* moss to colonize and grow, facilitating the increase in sphagnicolous rhizopods.

The most apparent feature defining pollen subzone P-3b is a doubling in the percentage of *Alnus* pollen above 7 cm (figure 4.2) corresponding to a date of AD 1972 (BP -22 ± 3). The gravel road connecting Port Clements to Masset in 1958 opened this region to large scale clear-cut logging. Alder is one of the first trees to colonize following disturbance events that open up the forest canopy in this region. The alder pollen signal appears slightly delayed which is to be expected as the trees require time to colonize and mature.

### *5.2.2. Deer Introduction*

Sitka black-tailed deer (*Odocoileus hemionus sitkensis*) were introduced to Graham Island in the early 1900s (Dalzell 1968), and are now the major large herbivore on the island. The decline in *Empetrum/Rhododendron* pollen and some of the herbaceous plants at the top of the core may be due to overgrazing (Gaston *et al.* 2008). Declines in ericaceous shrubs such as salal (*Gaultheria shallon*) and red huckleberry (*Vaccinium parvifolium*) as well as bog dwelling cloudberry (*Rubus chamaemorus*) have been specifically attributed to an overabundance of deer (B.C. Parks 1992). Anecdotal observation suggests that deer are currently active around Drizzle Bog as fresh droppings were observed on a number of occasions

## 5.3. Pollen Productivity and Climate

The pollen accumulation rate (PAR) is a measure of the number of pollen grains accumulated on a given surface area ($cm^2$) for a given period of time (1 year). The pollen concentration is an important component when determining the PAR and depends on the amount of pollen deposited by vegetation in the area as well as the rate of peat bog growth. If we can determine that certain cores, or sections of cores, have relatively constant accumulation rates, it follows that significant changes to PARs indicate changes in pollen production of regional vegetation. For this reason Middeldorp (1982) proposed the use of pollen concentration as a method for quantifying past net organic productivity.

Two factors that affect pollen deposition values are; 1) changes in the abundance of tree species contributing to the pollen record and 2) the size of the opening in forest

cover where deposition takes place (Hicks *et al.* 2004). While pollen deposition varies throughout the core, the main period of interest to this study concerning PAR is the last 200 years. Other than logging after ~ AD 1950 it seems reasonable to assume that both of these factors have remained relatively constant for this time period.

From a physiological standpoint, pollen production of conifer trees is a possible proxy for summer temperatures. Male cones are formed in late summer of the year preceding their release (Jalkanen *et al.* 2008). A study of conifer PAR by Huusko and Hicks (2009) found that pollen productivity is strongly correlated with July and August temperatures of the preceding year. The finest resolution in the Drizzle Bog core is 3 years $cm^{-1}$ and it is thus unreasonable to tease out annual changes. However, multi-year to decadal changes in climate, especially summer temperature, should be apparent in the record (figure 5.1).

During prolonged periods of cool summers reduced soil temperatures and metabolic rates due to lower temperatures and/or reduced photosynthesis rates from increased cloud cover may lead to a decrease in primary productivity, manifesting in lower pollen production. Under warm summer conditions we would expect the opposite with comparatively higher pollen production due to higher metabolic rate and longer growing seasons.

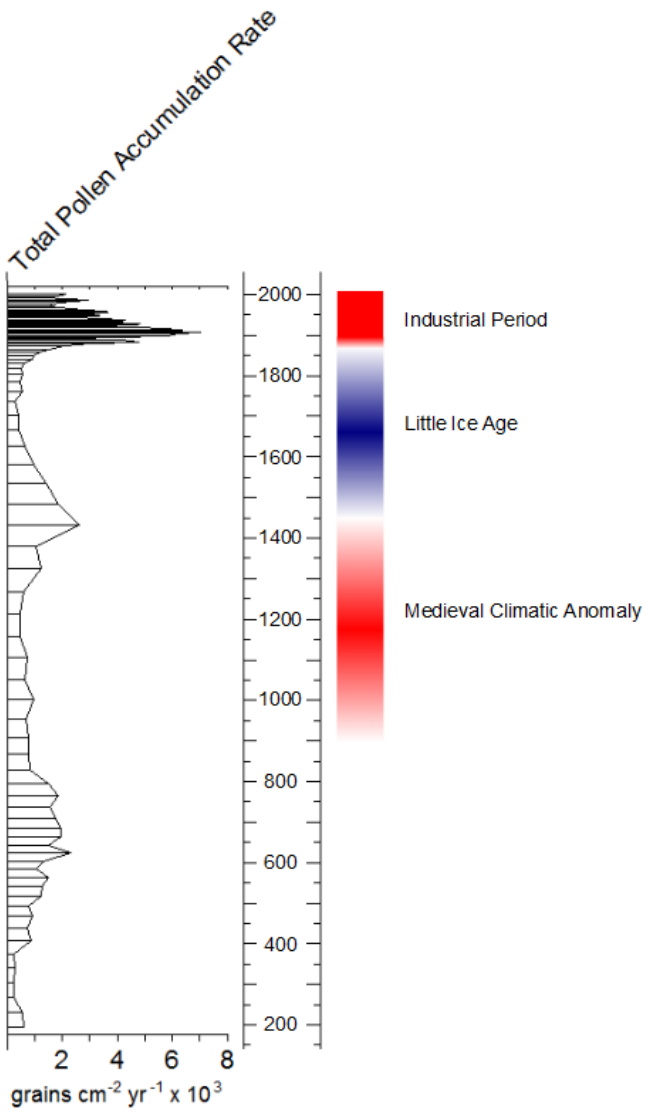


***Figure 5.1.*** ***Total Pollen Accumulation Rate (grains $cm^{-2}$ $yr^{-1}$ x $10^3$) compared with major climate events during the last 1800 years. Timeline is in calibrated years (AD).***

### *5.3.1. Pollen Accumulation Rate in Pollen Zone P-1*

Pollen zone P-1 spans the lower half of the core (45.5 to 90 cm) with two apparent periods of low pollen accumulation. The first period of low PAR is near the bottom of the core spanning 84-87 cm corresponding to between BP 1680 and 1580 (AD 270 and 370 ± 110). This time span displays the lowest PAR of the entire core at <300 grains $cm^{-2}$ $yr^{-1}$. The next period displaying low PAR is 56-65 cm spanning BP 1115-745 (AD 835-1205 ± 100). This encompasses subzone P-1b and notably displays the

accumulation of almost no *Sphagnum* spores. While not as low as the first low period, total PARs are still substantially lower than 1000 grains $cm^{-2}$ $yr^{-1}$.

A number of independent regional proxy climate records suggest regional cooling from BP 1550-1250 (AD 400-700; Hu *et al.* 2001; Reyes *et al.* 2006; Jackson *et al.* 2008). These estimates lie between the two periods of low pollen accumulation suggesting that cool temperatures were not the primary driver during these time intervals. As these two intervals are lower in the core it is possible that poor fen communities are less conducive to interpreting changes in pollen accumulation than mire communities with strictly ombrotrophic inputs.

### *5.3.2. Medieval Climatic Anomaly Productivity*

As previously discussed, the Medieval Climatic Anomaly (MCA) was a period of generally warmer and drier conditions from ~ BP 1050-500 (AD 900-1450) throughout the Northern Hemisphere. Regionally, the Pacific north-west and Gulf of Alaska appear to have experienced warmer and drier conditions during the MCA. Glacier retreat throughout Alaska appears to have occurred BP 650-500 (AD 1300-1450; Wiles *et al.* 2004). Coastal Alaskan glaciers show a similar trend but appear to end earlier by the early 1400s (Calkin *et al.* 2001). Tree-ring records from Prince William Sound suggest two multi-decadal warm periods centered around BP 650 and 510 (AD 1300 and 1440; Barclay *et al.* 1999). Perhaps the most interesting climate proxy comes from Yukon where ice cores from the St. Elias Mountains record increased fire activity from BP 710-540 (AD 1240-1410; Yalcin *et al.* 2006). Increased regional fire activity implies not only warmer summer temperatures but also prolonged dry periods not seen at any other time in the ice core record for the last 1000 years (Yalcin *et al.* 2006).

In the Drizzle Bog peat core the recurrence surface implied by the bulk density change and three-fold increase in pollen concentration at 52 cm appear to coincide with this regional dry period at ~ BP 550 (AD 1400 ± 100). The elevated pollen concentration along with the peak in ash content percentage may also indicate a hiatus in peat growth, though the precise length of this hiatus cannot be determined. In conjunction, climatic conditions in Alaska and Yukon appear to favor glacial retreat, increased tree-ring growth and high fire activity from ~ BP 650 to 500 (AD 1300-1450). These drier conditions

likely correspond with the pollen concentration spike which itself appears to occur between BP 650 and 450 (AD 1300 and 1500). This apparent dry period is followed by a prolonged period of cool summers indicated by low PARs suggesting a transition to Little Ice Age climatic conditions.

### *5.3.3. Little Ice Age Productivity*

The majority of studies describing Little Ice Age (LIA) climate impacts throughout the northern hemisphere suggest periodic cool intervals between BP 500 and 50 (AD 1450 and 1900; Fisher *et al*. 1983; Wiles *et al.* 1999; Calkin *et al.* 2001; Bradley *et al.* 2003; Mann and Jones 2003). While global mean annual temperatures were reduced, ice core data from the Canadian High Arctic suggests that summer cooling may have been even greater than the drop in mean annual temperature (Fisher *et al.* 1983).

The most recent period of low PARs in the Drizzle Bog core spans 48 to 35 cm with an age estimate of BP 350 to 75 (AD 1600 to 1875). Given the assumption that low total PAR is a proxy for cool summer temperatures, in this case below 1000 grains $cm^{-2}$ $yr^{-1}$, climatic conditions during the Little Ice Age appear to greatly reduce the regional pollen productivity of vegetation on and around Drizzle Bog.

Given the proposed influences of LIA climate on summer temperature, cold-adapted species are likely to have fared better over this period. This appears to be the case as *Empetrum* (*Empetrum/Rhododendron* type) shows a spike in pollen percentage spanning this time period. *Empetrum nigrum* is a dwarf shrub with a circumpolar distribution inhabiting a range of habitats from lowland *Sphagnum* bogs to subalpine regions on Haida Gwaii (Calder and Taylor 1968). It is likely that this wide tolerance range allows for *E. nigrum* to cope with cool temperatures better than many of the other species in the CWHwh1 zone that contribute to the regional pollen rain. *Empetrum* only shows a slight increase in PAR, but displays a high proportional change in pollen productivity when compared to other taxa.

The timing of the LIA in the core compares reasonably well with other regional studies. Coast mountain glaciers appear to have been at or near their maximum extent of the entire Holocene during this time (Desloges and Ryder 1990) which the authors attributed to prolonged periods of below-average temperatures and/or well above

average precipitation. Most of these Coast Mountain glaciers reached their maximum extent around BP 75 (AD 1875) followed by glacier retreat.

Tree-ring accounts recording warm season temperatures (April-September) around the Gulf of Alaska record cool summers through much of this period with the coldest period occurring BP 160-130 (AD 1790-1820) with subsequent warming around BP 80 (AD 1870; Wiles *et al.* 1996). A tree-ring record of White Spruce at the elevational tree line in the Wrangell Mountains (Davi *et al.* 2003) suggested two cold periods occurring around BP 250 (AD 1700) and between BP 150 and 120 (AD 1800 and 1830) with warming after BP 100 (AD 1850).

This period of cool growing season conditions appears to have had a significant impact on regional pollen productivity. The low pollen accumulation from ~ BP 450 and 75 (AD 1600 and 1875), nearly the lowest in the entire core, contrasts sharply with the nearly five-fold pollen accumulation increase immediately following ~ BP 75 (AD 1875).

### *5.3.4. Industrial Period Productivity*

Dramatic changes within the Drizzle Bog core that could be linked to modern climatic warming begin to occur after BP 75 (AD 1875). The PAR of the Drizzle Bog core begins to increase at 36.5 cm where it exceeds 1000 grains $cm^{-2}$ $yr^{-1}$ for the first time since 50 cm which translates to over 300 years. The rate increases dramatically at 34.5 cm (1875 ± 20 yrs), peaking at >4500 grains $cm^{-2}$ $yr^{-1}$ (32 cm) around BP 65 (AD 1885 ± 15 yrs). This nearly five-fold increase in pollen productivity over the span of <30 years is a noteworthy observation as this corresponds with other studies describing dramatic northern hemisphere warming after ~ BP 80 (AD 1870; Wiles *et al*. 1996; Mann 2002; Wilson *et al.* 2006).

Arctic communities have displayed similar responses following the end of the LIA. Ice core data from the Agassiz and Devon ice caps from the Canadian High Arctic on the Queen Elizabeth Islands (Bradley 1990) suggests that following a final cold period in BP 130-90 (AD 1820-1860), summer temperatures dramatically increased. This 19$^{th}$ century warming is also evident with distinct changes to the diatom assemblage and increased productivity in adjacent sites of Ellesmere Island lakes (Douglas *et al.* 1994) which were attributed to longer growing seasons.

More regional examples of changes to biotic communities include lake cores from the northern Coast Mountains which show an increase in planktonic algae in the uppermost sediments (Clague and Mathewes 1996). Increases in lake productivity inferred from high *Pediastrum* algal colonies were attributed to warming and subsequent lengthening of the growing season. Changes to the diatom assemblage in the 19$^{th}$ and 20$^{th}$ centuries in a follow-up study were suggestive of longer growing seasons and higher lake temperatures (Clague *et al.* 2004).

An important result is that nearly all pollen taxa display an apparent rise in productivity following BP 75 (AD 1875), not just coniferous trees. This suggests a change in climatic conditions, likely longer growing seasons, favourable to all vegetation types. The effects of rising $CO_2$ concentrations, largely due to anthropogenic sources, is a possible alternative as a number of studies describe fertilization effects of $CO_2$ on vegetation (Jablonski *et al.* 2002; Ainsworth and Long 2005). However, while young trees reportedly grow faster and thus reach maturity quicker (Ladeau and Clark 2006), there is little to no response of $CO_2$ enrichment on mature natural forests (Nowak *et al.* 2004; Korner *et al.* 2005).

It is unfortunate that few palynological studies investigate pollen accumulation rates over the last ~200 years in fine resolution. Barnekow *et al.* (2008) describe a similar change in pollen accumulation from Swedish lake sediments. However, Barnekow attributes increased pollen deposition either to land-use changes in the region or an over-estimation of PAR at the surface. The most comparable study is from a fluvial system in northwestern Iberia by Desprat *et al.* (2003) describing a nearly identical increase in pollen accumulation after BP 90 (AD 1860). They suggest that recent warming and/or increasing $CO_2$ concentration most likely explain pollen production increases over the last ~150 years. Desprat *et al.*'s core describes the last ~3000 years and as the pollen accumulation is at its highest after BP 100 (AD 1850) they suggest that this recent period is the warmest of the last three millennia.

### *5.3.5. Pollen Productivity Implications*

The pollen accumulation changes during these past climatic regimes appear to be largely temperature dependent. The underlying mechanism for the changes in

temperature is ultimately driven by Northeast Pacific offshore climate regimes. Any changes in the frequency of the inter-annual patterns of the Pacific Decadal Oscillation and/or the El Nino/Southern Oscillation or past shifts in the overlying pressure systems of the Aleutian Low and North Pacific High could have contributed to some of the changes in pollen accumulation we see earlier in the core. Gedalof *et al.* (2002) suggest that the strength of the Aleutian Low may be the possible keystone to the inter-annual cycles in the north Pacific from tree-ring and coral proxy data, at least as far back as AD 1600.

The recent increase in pollen accumulation after ~ BP 75 (AD 1875) described from this isolated area suggests that climate warming is likely having a significant impact on regional pollen production. An indirect indicator of past pollen production is the timing of seasonal activities of plants. Trends in phenological change in Europe and North America clearly show a lengthening of the growing season (Menzel 2000; Sparks and Menzel 2002; Walther *et al.* 2002). Longer growing seasons result in increased primary productivity and a prolonged period of pollen production (Emberlin *et al.* 2002). Unfortunately reliable phenological records generally start AD 1900 or later in western North America (Beaubien and Freeland 2000), with scarce regional records for comparison. Direct records of daily aerial pollen concentrations also show recent increases but are even more constrained in time, starting only after 1974 (WHO 2003). Due to the limited window of our knowledge of pollen productivity, biologically significant changes due to recent warming are likely to have begun earlier than previously thought.

While human health implications are beyond the scope of this thesis, high pollen concentrations in the air can be a contributing factor to increases in allergic respiratory diseases (Beggs and Bambrick 2005; Shea et al. 2008). The results of this thesis suggest the possibility that comparatively high concentrations of airborne pollen contributing to these conditions may be an Industrial Period phenomenon. With further research on pollen accumulation targeting the last 200 years, a comparative baseline for future pollen productivity changes may be possible.

.

# 6. Conclusion

The primary objectives of this thesis were to provide a reconstruction of the Drizzle Bog core to infer changes in regional vegetation and peatland development allowing for comparisons with other regional paleoenvironmental reconstructions. The three primary factors that control peatland development, namely vegetation succession, human impact, and climate, all appear to have played a role.

The 90 cm core spanning ~1800 years records the successional stages of a hypermaritime peatland displaying transition from a slightly minerotrophic poor fen to an ombrotrophic raised bog. The autogenic driver of vegetation succession does not appear to play as strong a role as the allogenic factors of climate and anthropogenic impacts. The inherent isolation of Haida Gwaii results in direct human impact not playing a role until later in the core. Changes in peatland dynamics and microfossil assemblage due to road construction through Drizzle Bog are clearly apparent after BP -8 (AD 1958). The regional impact due to logging accessibility in the area is also suggested from the recent doubling of the proportion of *Alnus* pollen, which is a clear indicator of disturbance.

In relation to climate, few changes are evident before BP 550 (AD 1400) other than a period from ~ BP 1150-750 (AD 800-1200) where *Sphagnum* spore production appears to be nearly non-existent. Around BP 550 (AD 1400), during the Medieval Climatic Anomaly, a spike in pollen concentration along with a peak in acid-insoluble minerals suggests little to no peat growth, likely due to drier than normal conditions. The dry mire conditions coincide with other studies identifying high fire activity and glacier recession throughout the Yukon and Alaska. Following this dry period, Little Ice Age influences manifest as cool summers leading to low pollen productivity from ~ BP 350-100 (AD 1600-1850), inferred by low accumulation rates. After ~ BP 75 (AD 1875), pollen accumulation rates of all taxa increase dramatically corresponding with the end of the LIA and warming associated with the Industrial Period. This apparent increase in pollen productivity in the majority of identified vegetation types is unprecedented in the 1800

years recorded in the core. Climate warming appears to be the primary driver of the increases described from this isolated region. Further high-resolution research should be undertaken to determine if plant taxa from other regions display this dramatic rise in recent pollen production.

# References


Ainsworth EA, Long SP. 2005. What have we learned from 15 years of free-air CO2 enrichment (FACE)? A meta-analytic review of the responses of photosynthesis, canopy properties and plant production to rising CO2. The New Phytologist 165:351-71.

Aiken SG, Dallwitz MJ, Consaul LL, McJannet CL, Boles RL, Argus GW, Gillett JM, Scott PJ, Elven R, LeBlanc MC, Gillespie LJ, Brysting AK, Solstad H, Harris JG. 2007. Flora of the Canadian Arctic Archipelago: Descriptions, Illustrations, Identification, and Information Retrieval. NRC Research Press, National Research Council of Canada, Ottawa. Available from: http://nature.ca/aaflora/data. Accessed on April 2, 2012.

Allen MR, Goudie AS. 2005. Natural Climate Fluctuations. In: Goudie AS, editor. Encyclopedia of Global Change: (e-reference edition). Oxford University Press. Available from: http://www.oxford-globalchange.com/entry?entry=t178.e0304. Accessed on May 28, 2012.

Anderson DE. 1998. A reconstruction of Holocene climatic changes from peat bogs in north-west Scotland. Boreas 27.

Appleby PG, Oldfield F. 1978. The calculation of Lead-210 dates assuming a constant rate of supply of unsupported 210Pb to the sediment. Atomic Energy 5.

Appleby PG, Shotyk W, Fankhauser A. 1997. Lead-210 age dating of three peat cores in the Jura Mountains, Switzerland. Water, Air, and Soil Pollution 100:223-231.

Auer V. 1930. Peat Bogs in Southeastern Canada. Geological Survey of Canada Memoir 162, 32 p.

B.C. Parks. 1992. Naikoon Park master plan background document.

Barber KE. 1981. Peat Stratigraphy and Climate Change. Balkema, Rotterdam: Merrimack Book Service, Salem, N.H.

Barclay DJ, Calkin PE, Wiles GC. 1999. A 1119-year tree-ring-width chronology from western Prince William Sound, southern Alaska. The Holocene 9:79-84.

Barnekow L, Bragée P, Hammarlund D, St. Amour N. 2008. Boreal forest dynamics in north-eastern Sweden during the last 10,000 years based on pollen analysis. Vegetation History and Archaeobotany 17:687-700.

Beaubien EG, Freeland HJ. 2000. Spring phenology trends in Alberta, Canada: links to ocean temperature. International Journal of Biometeorology 44:53-59.

Beggs PJ, Bambrick HJ. 2005. Is the Global Rise of Asthma an Early Impact of Anthropogenic Climate Change? Environmental Health Perspectives 113:915-919.

Benninghof WS. 1962. Calculation of pollen and spores density. Pollen et Spores 4:332-333.

Birks HH, Birks HJB. 2006. Multi-proxy studies in palaeolimnology. Vegetation History and Archaeobotany 15:235-251.

Birks HJB, Birks HH. 1980. Quaternary Palaeoecology. London: Edward Arnold.

Birks HJB, Webb III T, Berti AA. 1975. Numerical analysis of pollen samples from central Canada: A comparison of methods. Review of Palaeobotany and Palynology 20:133-169.

Blaauw M. 2010. Methods and code for “classical” age-modelling of radiocarbon sequences. Quaternary Geochronology 5:512-518.

Blackford J. 2000. Palaeoclimatic records from peat bogs. Trends in Ecology & Evolution 15:193-198.

Booth RK, Jackson ST. 2003. A high-resolution record of late-Holocene moisture variability from a Michigan raised bog, USA. The Holocene 13:863-876.

Booth RK. 2001. Ecology of Testate Amoebae (Protozoa) in Two Lake Superior Coastal Wetlands: Implications for Paleoecology and Environmental Monitoring. Wetlands 21:564-576.

Bradley RS, Hughes MK, Diaz HF. 2003. Climate in Medieval time. Science 302:404-5.

Bradley RS. 1990. Holocene Paleoclimatology of the Queen Elizabeth Islands, Canadian High Arctic. Quaternary Science Reviews 9:365-384.

van Breeman N. 1995. How Sphagnum bogs down other plants. Trends in Ecology & Evolution 10.

Bronk Ramsey C. 2001. Development of the Radiocarbon Calibration Program. Radiocarbon 43:355-363.

Calder JA, Taylor RL. 1968. Flora of the Queen Charlotte Islands Part 1. Ottawa, Ontario: Queen’s Printer and Controller of Stationary.

Calkin PE, Wiles GC, Barclay DJ. 2001. Holocene coastal glaciation of Alaska. Quaternary Science Reviews 20:449-461.

Chambers FM, Beilman DW, Yu Z. 2011. Methods for determining peat humification and for quantifying peat bulk density, organic matter and carbon content for palaeostudies of climate and peatland carbon dynamics. Mires and Peat 7:1-10.

Chambers FM, Charman DJ. 2004. Holocene environmental change: contributions from the peatland archive. The Holocene 14:1-6.

Charman DJ. 2001. Biostratigraphic and palaeoenvironmental applications of testate amoebae. Quaternary Science Reviews 20:1753-1764.

Clague JJ, Mathewes RW. 1996. Neoglaciation, Glacier-Dammed Lakes, and Vegetation Change in Northwestern British Columbia, Canada. Arctic and Alpine Research 28:10-24.

Clague JJ, Wohlfarth B, Ayotte J, Eriksson M, Hutchinson I, Mathewes RW, Walker IR, Walker L. 2004. Late Holocene environmental change at treeline in the northern Coast Mountains, British Columbia, Canada. Quaternary Science Reviews 23:2413-2431.

Clymo RS, Hayward PM. 1982. The Ecology of Sphagnum. In: Smith AJE, editor. Bryophyte Ecology. New York: Chapman and Hall Ltd. pp. 229-290.

Dalzell KE. 1968. The Queen Charlotte Islands 1774-1966. Terrace, B.C.: C.M. Adam

Davi NK, Jacoby GC, Wiles GC. 2003. Boreal temperature variability inferred from maximum latewood density and tree-ring width data, Wrangell Mountain region, Alaska. Quaternary Research 60:252-262.

DellaSala DA, Moola F, Alaback P, Paquet P, Schoen JW, Noss RF. 2011. Temperate and Boreal Rainforests of the Pacific Coast of North America. In: DellaSalla DA, editor. Temperate and Boreal Rainforests of the World: Ecology and Conservation. Washington, DC: Island Press.

Denton GH, Karlen W. 1973. Holocene Climatic Variations - Their Pattern and Possible Cause. Quaternary Research 3:155-205.

Desloges JR, Ryder JM. 1990. Neoglacial history of the Coast Mountains near Bella Coola, British Columbia. Canadian Journal of Earth Sciences 27:281-290.

Desprat S, Sánchez Goñi MF, Loutre M-F. 2003. Revealing climatic variability of the last three millennia in northwestern Iberia using pollen influx data. Earth and Planetary Science Letters 213:63-78.

Douglas MSV, Smol JP, Blake Jr. W. 1994. Marked Post-18th century environmental change in high-arctic ecosystems. Science 266:416-419.

Edwards AWF, Cavalli-Sforza LL. 1964. Reconstruction of evolutionary trees. In: Heywood VH, McNeill J, editors. Phenetic and phylogenetic classification: Systematic Assoc. Publ. 6. pp. 67-76.

Emberlin J, Detandt M, Gehrig R, Jaeger S, Nolard N, Rantio-Lehtimäki A. 2002. Responses in the start of Betula (birch) pollen seasons to recent changes in spring temperatures across Europe. International journal of biometeorology 46:159-70.

Environment Canada. 2011. Canadian Climate Normals. Available from: http://www.climate.weatheroffice.gc.ca/climate_normals/index_e.html. Accessed October 4, 2011

Faegri K, Kaland PE, Krzywinski K. 1989. Textbook of Pollen Analysis. 4th ed. London: Alden Press.

Fiacco Jr. RJ, Palais JM, Germani MS, Zielinski GA, Mayewski PA. 1993. Characteristics and possible source of a 1479 AD volcanic ash layer in a Greenland Ice Core. Quaternary Research 39:267-273.

Fisher DA, Koerner RM, Paterson WSB, Dansgaard W, Gundestrup N, Reeh N. 1983. Effect of wind scouring on climatic records from ice-core oxygen-isotope profiles. Nature 301.

Foster JB. 1989. Conservation in the Queen Charlotte Islands. In: Scudder GGE, Gessler N, editors. The Outer Shores. Skidegate: Queen Charlotte Islands Museum Press. pp. 281-302.

Fritz SC. 2003. Lacustrine perspectives on Holocene climate. In: Mackay A, Battarbee R, Birks J, Oldfield F, editors. Global Change in the Holocene. New York: Oxford University Press. pp. 227-241.

Gaston AJ, Golumbia TE, Martin JL, Sharpe ST. 2008. Lessons from the Islands: Introduced species and what they tell us about how ecosystems work. Ottawa

Gedalof Z, Mantua NJ, Peterson DL. 2002. A multi-century perspective of variability in the Pacific Decadal Oscillation: new insights from tree rings and coral. Geophysical Research Letters 29

van Geel B. 1972. Palynology of a section from the raised peat bog “Wietmarscher Moor”, with special reference to fungal remains. Acta Botanica Neerlandica 21:261-284.

van Geel B. 1976. A Paleoecological study of Holocene peat bog sections, based on the analysis of pollen, spores and macro- and microscopic remains of fungi, algae, cormophytes and animals. Amsterdam: Hugo de Vries Laboratorium Universiteit

Gignac LD, Vitt DH, Zoltap SC, Bayley SE. 1991. Bryophyte response surfaces along climatic, chemical, and physical gradients in peatlands of western Canada. Nova Hedwigia 53.

Gignac LD, Vitt DH. 1990. Habitat Limitations of Sphagnum along Climatic, Chemical, and Physical Gradients in Mires of Western Canada. The Bryologist 93:7-22.

Gignac LD, Vitt DH. 1994. Responses of northern peatlands to climate change: effects on bryophytes. J. Hattori Bot. Lab. 75:119-132.

Gignac LD. 2001. Bryophytes as Indicators of Climate Change. The Bryologist 104:410-420.

Givelet N, Le Roux G, Cheburkin A, Chen B, Frank J, Goodsite ME, Kempter H, Krachler M, Noernberg T, Rausch N, et al. 2004. Suggested protocol for collecting, handling and preparing peat cores and peat samples for physical, chemical, mineralogical and isotopic analyses. Journal of environmental monitoring : JEM 6:481-92.

Glime JM. 2007. Bryophyte Ecology. Volume 2. Bryological Interaction. Ebook sponsored by Michigan Technological University and the International Association of Bryologists. Accessed on Feb 28, 2012.

Google Maps. 2012. Google, Haida Gwaii. Available from: http://maps.google.com. Accessed on April 26, 2012.

Green RN, Klinka K. 1994. Land Management Handbook 28: A Field Guide for Site Identification and Interpretation for the Vancouver Forest Region. Victoria, B.C.

Grimm EC. 1987. CONISS: A FORTRAN 77 Program for Stratigraphically Constrained Cluster Analysis by the Method of Incremental Sum of Squares. Computers & Geosciences 13:12-35.

Grimm EC. 2011. TILIA v1.7 (computer software).

Grove JM. 1988. The Little Ice Age. New York: Methuen & Co.

Guijarro JA. 2011. climatol: Some Tools for Climatology: series homogenization, plus windrose and Walter&Lieth diagrams. R package version 2.1.

Hebda RJ. 1977. The Paleoecology of a raised bog and associated deltaic sediments of the Fraser River Delta. 201 p.

Hebda RJ. 1979. Size, productivity, and paleoecological implications of ericaceous pollen from Burns Bog, southern Fraser River Delta, British Columbia. Canadian Journal of Botany 57.

Herweijer C, Seager R, Cook ER, Emile-Geay J. 2007. North American Droughts of the Last Millennium from a Gridded Network of Tree-Ring Data. Journal of Climate 20:1353-1376.

Heusser CJ. 1955. Pollen profiles from the Queen Charlotte Islands, British Columbia. Canadian Journal of Botany 33.

Heusser CJ. 1960. Late-Pleistocene environments of North Pacific North America. American Geographic Society Special Publication. 35

Hicks S, Goslar T, Borg K van der. 2004. A near annual record of recent tree-line dynamics from northern Finland. Acta Palaeobotanica 44:299-316.

Hu FS, Ito E, Brown TA, Curry BB, Engstrom DR. 2001. Pronounced climatic variations in Alaska during the last two millennia. Proceedings of the National Academy of Sciences of the United States of America 98:10552-6.

Huusko A, Hicks S. 2009. Conifer pollen abundance provides a proxy for summer temperature : evidence from the latitudinal forest limit in Finland. October 24:522-528.

IPCC. 2007. Climate Change 2007 : Contribution of Working Groups I, II and III to the Fourth Assessment Report of the Intergovernmental Panel on Climate Change. Cambridge, United Kingdom

ITIS. 2012. Integrated Taxonomic Information System on-line database. Available from: http://www.itis.gov

Jablonski LM, Wang X, Curtis PS. 2002. Plant reproduction under elevated CO2 conditions: a meta-analysis of reports on 79 crop and wild species. New Phytologist 156:9-26.

Jackson SI, Laxton SC, Smith DJ. 2008. Dendroglaciological evidence for Holocene glacial advances in the Todd Icefield area, northern British Columbia Coast Mountains. Canadian Journal of Earth Sciences 45:83-98.

Jalkanen R, Hicks S, Aalto T, Salminen H. 2008. Past pollen production reconstructed from needle production in Pinus sylvestris at the northern timberline: a tool for evaluating palaeoclimate reconstructions. Silva Fennica 42:499-513.

Jones PD, New M, Parker DE, Martin S, Rigor IG. 1999. Surface air temperature and its changes over the past 150 years. Reviews of Geophysics 37:173.

Jones PD, Briffa KR, Osborn TJ, Lough JM, van Ommen TD, Vinther BM, Luterbacher J, Wahl ER, Zwiers FW, Mann ME, et al. 2009. High-resolution palaeoclimatology of the last millennium: a review of current status and future prospects. The Holocene 19:3-49.

Kapp RO, Davis OK, King JE. 2000. Pollen and Spores. 2nd ed. College Station, TX: The American Association of Stratigraphic Palynologists

Kinchin IM. 1994. The Biology of Tardigrades. London: Blackwell Publishing Co.

Koch J, Clague JJ. 2011. Extensive glaciers in northwest North America during Medieval time. Climatic Change 107:593-613.

Körner C, Asshoff R, Bignucolo O, Hättenschwiler S, Keel SG, Peláez-Riedl S, Pepin S, Siegwolf RTW, Zotz G. 2005. Carbon flux and growth in mature deciduous forest trees exposed to elevated CO2. Science 309:1360-2.

Ladeau SL, Clark JS. 2006. Pollen production by Pinus taeda growing in elevated atmospheric CO 2. Functional Ecology 20:541-547.

Lamb HH. 1995. Climate, History and the Modern World. 2nd ed. New York: Routledge

Leary D. 1982. More Road Building on Graham Island. In: Simpson SL, editor. Tales from the Queen Charlotte Islands Book 2. Masset, B.C.: Senior Citizens of the Queen Charlotte Islands. pp. 55-58.

Luckman BH. 1986. Reconstruction of Little Ice Age Events in the Canadian Rocky Mountains. Geographie physique et Quaternaire XL:17-28.

MacKenzie WH, Moran JR. 2004. Wetlands of British Columbia: a guide to identification. Land Manag. Victoria, BC: Province of British Columbia

Mann ME, Jones PD. 2003. Global surface temperatures over the past two millennia. Geophysical Research Letters 30:15-18.

Mann ME. 2002. The value of multiple proxies. Science 297:1481-1482.

Manten AA. 1967. Lennart von Post and the Foundation of Modern Palynology. Review of Palaeobotany and Palynology 1:11-22.

Mantua NJ, Hare SR, Zhang Y, Wallace JM, Francis RC. 1997. A Pacific interdecadal climate oscillation with impacts on salmon production. Bulletin of the American Meteorological Society 78:1069-1079.

Mathewes RW. 1989. Paleobotany of the Queen Charlotte Islands. In: Scudder GGE, Gessler N, editors. The Outer Shores. Skidegate: Queen Charlotte Islands Museum. pp. 75-90.

McAndrews JH, Berti AA, Norris G. 1973. Key to the Quaternary Pollen and Spores of the Great Lakes Region. Toronto, Ontario: Royal Ontario Museum

McQueen CB. 1985. Spore Morphology of Four Species of Sphagnum in Section Acutifolia. The Bryologist 88:1-4.

Menounos B, Osborn G, Clague JJ, Luckman BH. 2009. Latest Pleistocene and Holocene glacier fluctuations in western Canada. Quaternary Science Reviews 28:2049-2074.

Menzel A. 2000. Trends in phenological phases in Europe between 1951 and 1996. International Journal of Biometeorology 44:76-81.

Middeldorp AA. 1982. Pollen Concentration as a Basis for Indirect Dating and Quantifying Net Organic and Fungal Production in a Peat Bog Ecosystem. Review of Palaeobotany and Palynology 37:225-282.

Moore PD, Bellamy DJ. 1973. Peatlands. London: Paul Elek (Scientific Books) Ltd

Moore PD, Webb JA, Collinson ME. 1991. Pollen Analysis. 2nd ed. Blackwell Scientific Publications

Nowak RS, Ellsworth DS, Smith SD. 2004. Functional responses of plants to elevated atmospheric CO2- do photosynthetic and productivity data from FACE experiments support early predictions? New Phytologist 162:253-280.

Ogden CG, Hedley RH. 1980. An Atlas of Freshwater Testate Amoebae. New York: Oxford University Press

Payne RJ, Lamentowicz M, der Knaap WOV, van Leeuwen JFN, Mitchell EAD, Mazei Y. 2012. Testate amoebae in pollen slides. Review of Palaeobotany and Palynology 173:68-79.

Piotrowska N, Blaauw M, Mauquoy D, Chambers FM. 2011. Constructing deposition chronologies for peat deposits using radiocarbon dating. Mires and Peat 7:1-14.

Pojar J, MacKinnon A, Alaback P, Antos J, Goward T, Lertzman K, Pojar R, Reed A, Turner N, Vitt DH. 1994. Plants of coastal British Columbia. (Pojar J, MacKinnon A, editors.). Vancouver: Lone Pine Publishing

von Post L. 1946. The prospect for pollen analysis in the study of the Earth's climatic history. Ymer:193-217.

Quickfall GS. 1987. Paludification and Climate on the Queen Charlotte Islands during the past 8000 years. 99 p.

R Development Core Team. 2011. R: A language and environment for statistical computing (software program).

Reimer PJ, Baillie MGL, Bard E, Bayliss A, Beck JW, Blackwell PG, Bronk Ramsay C, Buck CE, Burr GS, Edwards RL, et al. 2009. INTCAL09 and MARINE09 radiocarbon age calibration curves, 0-50,000 years cal BP. Radiocarbon 51:1111-1150.

Reyes AV, Wiles GC, Smith DJ, Barclay DJ, Allen S, Jackson S, Larocque S, Laxton S, Lewis D, Calkin PE, et al. 2006. Expansion of alpine glaciers in Pacific North America in the first millennium A.D. Geology 34:57.

Le Roux G, Marshall WA. 2011. Constructing recent peat accumulation chronologies using atmospheric fall-out radionuclides. Mires and Peat 7:1-14.

Rydin H, Jeglum JK, Hooijer A. 2006. The biology of peatlands. Oxford; New York: Oxford University Press

Siebert L, Simkin T. 2002-2012. Volcanoes of the World: an Illustrated Catalog of Holocene Volcanoes and their Eruptions. Smithsonian Institution, Global Volcanism Program, Digital Information Series, GVP-3. Available from: http://www.volcano.si.edu/world/. Accessed February 10, 2012.

Shea KM, Truckner RT, Weber RW, Peden DB. 2008. Climate change and allergic disease. The Journal of allergy and clinical immunology 122:443-53.

Sparks TH, Menzel A. 2002. Observed changes in seasons: an overview. International Journal of Climatology 22:1715-1725.

Steinmann P, Shotyk W. 1997. Geochemistry, mineralogy, and geochemical mass balance on major elements in two peat bog profiles (Jura Mountains, Switzerland). Chemical Geology 138:25-53.

Stine S. 1994. Extreme and persistant drought in California and Patagonia during mediaeval time. Nature 369.

Tallis JH. 1962. The identification of Sphagnum spores. Transactions of the British Bryological Society 4.

Taylor WT, Sanders RW. 2001. Protozoa. In: Thorp J, Covich A, editors. Ecology and Classification of North American Freshwater Invertebrates. 2nd ed. Academic Press. pp. 43-96.

Terasmae J. 1955. On the Spore Morphology of Some Sphagnum Species. The Bryologist 58:306-311.

Thomson RE. 1989. The Queen Charlotte Islands Physical Oceanography. In: Scudder GGE, Gessler N, editors. The Outer Shores. Skidegate: Queen Charlotte Islands Museum. pp. 75-90.

Tolonen K, Warner BG, Vasander H. 1992. Ecology of testaceans (Protozoa, Rhizopoda) in mires in Southern Finland. Archiv Fur Protistenkunde 142:119-138.

Turetsky MR, Manning SW, Wieder RK. 2004. Dating recent peat deposits. Wetlands 24:324-356.

Verhoeven JTA, Liefveld WM. 1997. The ecological significance of organochemical compounds in Sphagnum. Acta Botanica Neerlandica 6:117-130.

Vitt DH, Chee W-L. 1990. The relationships of vegetation to surface water chemistry and peat chemistry in fens of Alberta, Canada. Vegetatio 89:87-106.

Vitt DH. 1994. An Overview of Factors that influence the Development of Canadian Peatlands. Memoirs of the Entomological Society of Canada 169:7-20.

WHO. 2003. Phenology and Human Health: Allergic Disorders. WHO Regional Office for Europe. Copenhagen, Denmark

Walker IR, Pellatt MG. 2003. Climate Change in Coastal British Columbia — A Paleoenvironmental Perspective. Canadian Water Resources Journal 28:531-566.

Walther G-R, Post E, Convey P, Menzel A, Parmesank C, Beebee TJC, Fromentin J-M, Hoegh-guldberg O, Bairlein F. 2002. Ecological responses to recent climate change. Nature 416:389-395.

Wardenaar ECP. 1987. A new hand tool for cutting peat profiles. Canadian Journal of Botany 65:1772-1773.

Warner BG, Clague JJ, Mathewes RW. 1984. Geology and Paleoecology of a Mid-Wisconsin Charlotte Islands, British Columbia, Peat from the Queen Charlotte islands, British Columbia, Canada. Quaternary Research 21:337-350.

Warner BG, Bunting MJ. 1996. Indicators of rapid environmental change in northern peatlands. In: Berger AR, Iams WJ, editors. Geoindicators: Assessing Rapid Environmental Changes in Earth Systems. A.A. Balkema, Rotterdam. pp. 235–246.

Wiles GC, Barclay DJ, Calkin PE. 1999. Tree-ring-dated "Little Ice Age" histories of maritime glaciers from western Prince William Sound, Alaska. The Holocene 2:163-173.

Wiles GC, D'Arrigo RD, Jacoby GC. 1996. Temperature changes along the Gulf of Alaska and the Pacific Northwest coast modeled from coastal tree rings. Canadian Journal of Forest Research 26:474-281.

Wiles GC, D'Arrigo RD, Villalba R, Calkin PE, Barclay DJ. 2004. Century-scale solar variability and Alaskan temperature change over the past millennium. Geophysical Research Letters 31:2-5.

Wilson R, Wiles G, D'Arrigo R, Zweck C. 2006. Cycles and shifts: 1,300 years of multi-decadal temperature variability in the Gulf of Alaska. Climate Dynamics 28:425-440.

Yalcin K, Wake CP, Kreutz KJ, Whitlow SI. 2006. A 1000-yr record of forest fire activity from Eclipse Icefield, Yukon, Canada. The Holocene 16:200-209.

Yeloff D, Charman D, van Geel B, Mauquoy D. 2007. Reconstruction of hydrology, vegetation and past climate change in bogs using fungal microfossils. Review of Palaeobotany and Palynology 146:102-145.

# Appendices

# Appendix A.

## Vegetation transect data from Drizzle Bog

| Cover category | Species or type | w1 | w2 | w3 | w4 | w5 | e1 | e2 | e3 | e4 | e5 | n1 | n2 | n3 | n4 | n5 | s1 | s2 | s3 | s4 | s5 |
|---|---|---|---|---|---|---|---|---|---|---|---|---|---|---|---|---|---|---|---|---|---|
| **Trees** | *Pinus contorta* var *contorta* | 0 | 0.01 | 0.02 | 0.1 | 0 | 0 | 0 | 0 | 0 | 0 | 0.01 | p | p | 0 | 0.2 | p | 0 | 0.05 | 0.3 | 0 |
| | *Thuja plicata* | 0 | 0 | 0 | 0 | 0 | 0.05 | 0.3 | 0 | 0 | 0 | 0.5 | 0 | 0 | 0 | 0 | 0 | 0 | 0 | 0 | 0 |
| **Dwarf Shrubs and Herbs** | *Juniperus communis* | 0.05 | 0.1 | 0.4 | 0.3 | 0.25 | 0.1 | 0 | 0.02 | 0.05 | 0.1 | 0.2 | 0.1 | 0.02 | 0.1 | 0.1 | 0.1 | 0.07 | 0.07 | 0.01 | 0.1 |
| | *Vaccinium uliginosum* | 0.1 | 0.05 | 0.05 | p | 0 | 0.05 | 0.01 | 0.05 | 0.01 | 0 | p | 0.02 | p | 0.02 | 0.02 | 0.01 | 0.02 | 0.02 | 0.05 | 0.02 |
| | *Rhododendron groenlandicum* | 0.02 | 0.01 | 0.01 | 0.01 | 0.02 | p | p | p | p | p | 0.01 | p | p | 0.01 | p | p | 0.01 | 0.01 | p | 0.01 |
| | *Empetrum nigrum* | 0.1 | 0.1 | 0.3 | 0.2 | 0.3 | 0.03 | 0.01 | 0.08 | 0.05 | 0.2 | 0.05 | 0.07 | 0.05 | 0.07 | 0.1 | 0.1 | 0.15 | 0.15 | 0.2 | 0.05 |
| | *Cornus unalashkensis* | 0.01 | p | 0.01 | p | p | 0.01 | p | p | 0.01 | 0.01 | 0.01 | 0.01 | p | p | 0.01 | 0.02 | 0.01 | 0.02 | 0.05 | 0.01 |
| | *Kalmia microphylla* | p | p | p | 0.01 | p | p | p | 0.01 | p | p | p | 0.01 | 0.01 | 0.01 | 0.02 | 0.01 | p | p | p | p |
| | *Rubus chamaemorus* | 0.01 | 0.02 | 0.01 | 0.02 | 0.02 | 0.01 | 0.01 | 0.02 | 0.03 | 0.05 | p | 0.01 | 0.02 | 0.02 | 0.02 | 0.01 | p | 0.01 | 0.01 | 0.02 |
| | *Triantha glutinosa* | p | p | p | p | 0 | p | p | p | p | p | p | p | p | p | p | p | p | p | p | p |
| | *Nephrophyllidium crista-galli* | p | 0.01 | 0 | 0 | p | p | 0 | 0 | p | p | p | p | p | 0 | p | 0 | 0 | 0 | 0 | 0 |
| | *Sanguisorba officinalis* | 0 | p | p | 0.01 | 0 | p | 0 | p | p | 0 | p | 0 | p | p | p | 0 | p | p | p | 0 |
| | *Drosera rotundifolia* | 0 | p | p | p | p | p | 0.01 | p | 0 | p | p | 0 | p | p | p | p | p | p | p | p |
| | *Vaccinium oxycoccos* | 0 | 0 | 0 | 0 | 0 | 0.02 | 0 | 0.01 | 0 | 0.05 | p | 0.02 | 0.01 | p | p | p | p | p | p | 0.02 |
| | *Vaccinium caespitosum* | 0 | 0 | 0 | 0 | 0 | 0 | 0.01 | p | 0 | 0 | 0 | 0 | 0 | 0 | p | p | 0 | 0 | 0 | 0 |
| **Graminoids** | Cyperaceae | 0.01 | 0.02 | p | 0.03 | 0.02 | 0.08 | 0.05 | 0.02 | 0.02 | p | 0.05 | 0 | 0.05 | 0.01 | 0.05 | 0.05 | 0.15 | p | 0.01 | 0.05 |
| | Poaceae | 0 | 0 | 0 | 0 | 0 | 0 | 0.01 | 0 | 0 | 0 | 0 | 0 | 0 | 0 | 0 | 0 | 0 | 0 | 0 | 0 |
| **Bryophytes and Lichen** | *Sphagnum* spp. | 0.8 | 0.5 | 0.45 | 0.7 | 0.65 | 0.8 | 0.6 | 0.9 | 0.75 | 0.9 | 0.6 | 0.9 | 0.9 | 0.8 | 0.8 | 0.9 | 0.4 | 0.9 | 0.6 | 0.95 |
| | Lichen | 0.01 | 0.3 | 0.4 | 0.3 | 0.2 | 0.1 | 0 | 0.05 | 0.05 | 0.01 | 0.4 | 0.01 | 0.2 | 0.2 | 0.25 | 0.05 | 0.2 | 0.05 | 0.15 | 0.05 |
| | Non-sphagnum bryophytes | 0 | 0 | 0 | 0 | 0.01 | 0.01 | 0.02 | 0 | p | p | p | p | p | p | p | p | 0.1 | p | 0.1 | p |
| **Other** | Water | 0 | 0.05 | 0 | 0 | 0 | 0 | 0.1 | 0 | 0 | 0 | 0 | 0 | 0 | 0 | 0 | 0 | 0.1 | 0 | 0 | 0 |
| | Deer droppings | 0 | 0 | 0 | 0 | 0 | 0 | 0 | 0 | 0 | 0.02 | 0 | 0 | 0 | 0 | 0 | 0 | 0 | 0 | 0 | 0 |

Two 20 m intersecting transects were taken at the coring site. The first transect was oriented along a random compass bearing, with the second perpendicular to the first. 1 m x 1 m plots were assessed at 1 m intervals along each transect. The percentage cover of all identifiable species was recorded within each vegetation plot. (p) refers to present but less than 1 %.

# Appendix B.

## Microtephra

The search for microtephra was not a primary goal of the intended research but a peak in the ash content percentage (figure 4.1) combined with an apparent peak in Titanium trace elements (Shotyk, unpublished) led us to further investigate certain regions of the core. Glass shards resembling microtephra (figure B.1) were most abundant between 49 and 52 cm. The interpolated age range for the samples at this depth was between BP 533 and 385 (AD 1417 and 1565; 2 σ range AD 1323-1655). This led us to initially suspect the possibility of tephra from a series of Mount St. Helens eruptions beginning in BP 471-470 (AD 1479-1480). Glass shards matching this event have been found as far away as Greenland (Fiacco *et al.* 1993) so that finding tephra on Haida Gwaii originating in Washington State was a possibility.

A potential sample (QCI 48; 49.2 cm) was treated with 30% Hydrogen peroxide overnight before it was shipped to Dr. Franklin Foit at Washington State University for further analysis. Foit used back-scattered electron imaging to get a compositional map of the sample before using an electron microprobe to get a quantitative elemental analysis of the microtephra shards.

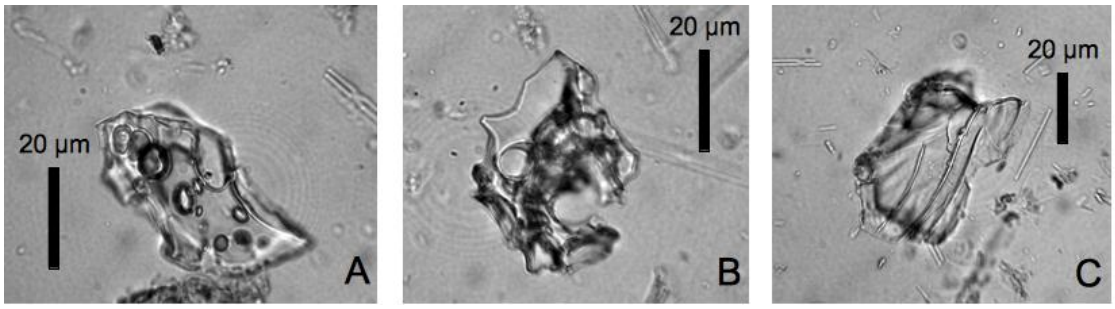


***Figure B.1. Pictures of microtephra***

The composition of 21 shards within the subsample was most similar to White River tephra deposits from the Mt. Churchill eruptions (BP 1887 and 1147; AD 63 and 803) with a similarity coefficient (SC) of 0.95. While the SC of the glass shards suggests a good match, some distinct differences in composition and the age discrepancy suggest

that the tephra is likely from another volcano in the region. Two other shards most resembled Mount St. Helens tephra (MSH Wn) from the BP 471-470 (AD 1479-1480) eruption (SC=0.93). This SC is too low to offer support for Mount St Helens tephra.

The microtephra results were largely inconclusive despite identifying two different glass shard compositions (F. Foit; personal communication; unreferenced). The interpolated ages of the samples are between BP 533 and 385 (AD 1417 and 1565; 2σ error range AD 1323-1655), during which a number of regional volcanic events occurred. The eruption of two Alaskan volcanoes, Augustine volcano ( ~1400 km to the northwest) and Aniakchuk caldera (~1550 km to the northwest) occurred around AD 410 (AD 1540 ± 100) and AD 390 (AD 1560 ± 50) respectively (Siebert and Simkin 2002-2012). Mount St. Helens, 1100 km to the southeast, is the only other known volcanic event to fall within this timeframe, with a series of eruptions beginning in BP 471-470 (AD 1479-1480). While not an exact match, the glass composition of 21 shards was most similar to White River tephra deposits from Mt. Churchill eruptions in BP 1890 (AD 60 ± 200) and BP 1150 (AD 800 ± 100). Mt.Churchill is almost 1400 km to the north of Drizzle Bog and ~500 km east of Augustine volcano but there are not known to be any eruptions within the sample ages. Two shards had glass compositions similar to the Mount St. Helens tephra (MSH Wn) but were not close enough to be conclusive. Therefore, the microtephra found within the Drizzle Bog core does not appear to match any known tephra deposits, either in composition or chronology. It is possible that they derive from an unknown volcanic event, possibly in the St. Elias Mountains near Mt. Churchill based on similar tephra composition.

# Appendix C.

## Calibrated ages for each sample depth

| Depth (cm) | 2 S.D. max (BP) | 2 S.D. min (BP) | Calibrated Age (BP) | Calibrated Age (AD) |
|---|---|---|---|---|
| 0.50 | -49.7 | -54.7 | -52.0 | 2002.0 |
| 1.56 | -45.6 | -48.6 | -46.6 | 1996.6 |
| 2.62 | -40.6 | -42.6 | -41.9 | 1991.9 |
| 3.68 | -36.0 | -39.0 | -37.1 | 1987.1 |
| 4.74 | -30.5 | -34.5 | -32.1 | 1982.1 |
| 5.80 | -24.9 | -29.9 | -27.1 | 1977.1 |
| 6.86 | -19.8 | -25.8 | -22.5 | 1972.5 |
| 7.92 | -15.6 | -22.6 | -18.6 | 1968.6 |
| 8.98 | -11.2 | -19.2 | -15.6 | 1965.6 |
| 10.04 | -8.7 | -16.7 | -12.9 | 1962.9 |
| 11.10 | -6.4 | -14.4 | -10.3 | 1960.3 |
| 12.16 | -3.8 | -11.8 | -7.5 | 1957.5 |
| 13.22 | -0.8 | -8.8 | -4.4 | 1954.4 |
| 14.28 | 3.0 | -5.0 | -0.9 | 1950.9 |
| 15.34 | 7.1 | -0.9 | 2.6 | 1947.4 |
| 16.40 | 10.2 | 1.2 | 5.8 | 1944.2 |
| 17.46 | 13.7 | 4.7 | 8.9 | 1941.1 |
| 18.52 | 16.8 | 7.8 | 11.9 | 1938.1 |
| 19.58 | 20.3 | 10.3 | 15.0 | 1935.0 |
| 20.64 | 23.1 | 13.1 | 18.1 | 1931.9 |
| 21.70 | 26.4 | 16.4 | 21.5 | 1928.5 |
| 22.76 | 30.4 | 20.4 | 25.1 | 1924.9 |
| 23.82 | 34.2 | 23.2 | 28.8 | 1921.2 |
| 24.88 | 38.8 | 27.8 | 32.7 | 1917.3 |
| 25.94 | 42.8 | 31.8 | 36.9 | 1913.1 |
| 27.00 | 47.6 | 35.6 | 41.2 | 1908.8 |
| 28.06 | 51.8 | 39.8 | 45.5 | 1904.5 |
| 29.12 | 57.5 | 43.5 | 50.0 | 1900.0 |
| 30.18 | 63.5 | 47.5 | 54.9 | 1895.1 |
| 31.24 | 70.7 | 48.7 | 59.9 | 1890.1 |
| 32.30 | 78.3 | 50.3 | 64.6 | 1885.4 |
| 33.36 | 86.9 | 51.9 | 69.3 | 1880.7 |
| 34.42 | 97.9 | 53.9 | 74.4 | 1875.6 |

| Depth (cm) | 2 S.D. max (BP) | 2 S.D. min (BP) | Calibrated Age (BP) | Calibrated Age (AD) |
|---|---|---|---|---|
| 35.48 | 108.6 | 55.6 | 80.2 | 1869.8 |
| 36.54 | 120.6 | 57.6 | 87.1 | 1862.9 |
| 37.60 | 135.6 | 61.6 | 95.5 | 1854.5 |
| 38.66 | 151.3 | 66.3 | 105.8 | 1844.2 |
| 39.72 | 169.2 | 72.2 | 118.4 | 1831.6 |
| 40.78 | 191.6 | 80.6 | 133.5 | 1816.5 |
| 41.84 | 217.5 | 90.5 | 151.7 | 1798.3 |
| 42.90 | 245.2 | 105.2 | 173.2 | 1776.8 |
| 43.96 | 275.3 | 124.3 | 198.4 | 1751.6 |
| 45.02 | 309.1 | 148.1 | 227.8 | 1722.2 |
| 46.08 | 345.7 | 177.7 | 261.5 | 1688.5 |
| 47.14 | 384.2 | 212.2 | 299.3 | 1650.7 |
| 48.20 | 425.3 | 254.3 | 340.6 | 1609.4 |
| 49.26 | 472.7 | 296.7 | 385.0 | 1565.0 |
| 50.32 | 522.1 | 341.1 | 432.1 | 1517.9 |
| 51.38 | 573.2 | 388.2 | 481.3 | 1468.7 |
| 52.44 | 626.5 | 437.5 | 532.4 | 1417.6 |
| 53.50 | 681.1 | 488.1 | 584.7 | 1365.3 |
| 54.56 | 735.1 | 539.1 | 637.8 | 1312.2 |
| 55.62 | 789.9 | 590.9 | 691.4 | 1258.6 |
| 56.68 | 843.8 | 641.8 | 744.8 | 1205.2 |
| 57.74 | 897.5 | 693.5 | 797.8 | 1152.2 |
| 58.80 | 949.7 | 744.7 | 849.7 | 1100.3 |
| 59.86 | 1000.5 | 794.5 | 900.2 | 1049.8 |
| 60.92 | 1048.7 | 842.7 | 948.9 | 1001.1 |
| 61.98 | 1094.1 | 888.1 | 995.1 | 954.9 |
| 63.04 | 1135.6 | 930.6 | 1038.6 | 911.4 |
| 64.10 | 1175.1 | 972.1 | 1078.8 | 871.2 |
| 65.16 | 1210.5 | 1010.5 | 1115.5 | 834.5 |
| 66.22 | 1243.7 | 1046.7 | 1148.8 | 801.2 |
| 67.28 | 1272.9 | 1078.9 | 1179.1 | 770.9 |
| 68.34 | 1299.9 | 1108.9 | 1206.9 | 743.1 |
| 69.40 | 1324.8 | 1136.8 | 1232.6 | 717.4 |
| 70.46 | 1347.7 | 1161.7 | 1256.4 | 693.6 |
| 71.52 | 1369.5 | 1185.5 | 1278.8 | 671.2 |
| 72.58 | 1389.5 | 1207.5 | 1300.2 | 649.8 |
| 73.64 | 1409.6 | 1229.6 | 1320.9 | 629.1 |
| 74.70 | 1430.0 | 1253.0 | 1341.3 | 608.7 |
| 75.76 | 1449.8 | 1274.8 | 1361.9 | 588.1 |

| Depth (cm) | 2 S.D. max (BP) | 2 S.D. min (BP) | Calibrated Age (BP) | Calibrated Age (AD) |
|---|---|---|---|---|
| 76.82 | 1469.4 | 1298.4 | 1383.0 | 567.0 |
| 77.88 | 1490.2 | 1323.2 | 1404.9 | 545.1 |
| 78.94 | 1510.0 | 1349.0 | 1428.1 | 521.9 |
| 80.00 | 1531.5 | 1378.5 | 1453.0 | 497.0 |
| 81.06 | 1555.7 | 1408.7 | 1479.8 | 470.2 |
| 82.12 | 1582.4 | 1440.4 | 1509.0 | 441.0 |
| 83.18 | 1612.4 | 1472.4 | 1540.2 | 409.8 |
| 84.24 | 1646.7 | 1505.7 | 1573.2 | 376.8 |
| 85.30 | 1681.8 | 1536.8 | 1607.7 | 342.3 |
| 86.36 | 1716.9 | 1562.9 | 1643.3 | 306.7 |
| 87.42 | 1754.2 | 1586.2 | 1679.8 | 270.2 |
| 88.48 | 1805.3 | 1606.3 | 1716.9 | 233.1 |
| 89.54 | 1857.9 | 1626.9 | 1754.3 | 195.7 |